Favreau *et al*., 2022 bioRxiv doi: https://doi.org/10.1101/2022.09.16.508090

Molecular Acclimation of *Halobacterium salinarum* to Halite Brine Inclusions

C. Favreau[1], A. Tribondeau[2], M. Marugan[1], F. Guyot[3], B. Alpha-Bazin[4], A. Marie[1], R. Puppo[1], T. Dufour[5], A. Huguet[6], S. Zirah[1], A. Kish[1*]

[1]Unité Molécules de Communication et Adaptation des Microorganismes (MCAM), Muséum National d'Histoire Naturelle (MNHN), CNRS, 57 rue Cuvier, 75005 Paris; France

[2]Unité Physiologie Moléculaire et Adaptation (PhyMA), MNHN, CNRS, 57 rue Cuvier, 75005 Paris; France

[3]Institut de Minéralogie, de Physique des Matériaux et de Cosmochimie (IMPMC), MNHN, Sorbonne Université, CNRS, IRD, 4 place Jussieu, 75005 Paris; France

[4] Département Médicaments et Technologies pour la Santé (DMTS), Université Paris-Saclay, CEA, INRAE, SPI, 30200 Bagnols-sur-Cèze; France

[5]Laboratoire de Physique des Plasma (LPP), Sorbonne Université, CNRS, Ecole Polytechnique, Université Paris-Sud, Observatoire de Paris, 4 Place Jussieu, 75252 Paris; France

[6]Unité Milieux Environnementaux Transferts et Interactions dans les hydrosystèmes et les Sols (METIS), Sorbonne Université, CNRS, EPHE, PSL 4 place Jussieu, 75005 Paris; France

*** Correspondence:**
Adrienne Kish, Unité MCAM, Muséum National d'Histoire Naturelle (MNHN), CNRS, 57 rue Cuvier, 75005 Paris; France
adrienne.kish@mnhn.fr

Keywords: *Halobacterium*, halophile, halite, proteomics

1 Abstract

Halophilic microorganisms have long been known to survive within the brine inclusions of salt crystals, as evidenced by the change in color for salt crystals containing pigmented halophiles. However, the molecular mechanisms allowing this survival has remained an open question for decades. While protocols for the surface sterilization of halite (NaCl) have enabled isolation of cells and DNA from within halite brine inclusions, "-omics" based approaches have faced two main technical challenges: (1) removal of all contaminating organic biomolecules (including proteins) from halite surfaces, and (2) performing selective biomolecule extractions directly from cells contained within halite brine inclusions with sufficient speed to avoid modifications in gene expression during extraction. In this study, we present methods to resolve these two technical challenges. In addition, we apply these methods to perform the first examination of the early acclimation of a model haloarchaeon

(*Halobacterium salinarum* NRC-1) to halite brine inclusions. Examinations of the proteome of *Halobacterium* cells two months post-evaporation revealed a high degree of similarity with stationary phase liquid cultures, but with a sharp down-regulation of ribosomal proteins. Low quantities of RNA from halite brine inclusions corroborate the hypothesis of low transcriptional and translational activities. While proteins for central metabolism were part of the shared proteome between liquid cultures and halite brine inclusions, proteins involved in cell mobility (archaellum, gas vesicles) were either absent or less abundant in halite samples. Proteins unique to cells within brine inclusions included transporters, suggesting modified interactions between cells and the surrounding brine inclusion microenvironment. The methods and hypotheses presented here enable future studies of the survival of halophiles in both culture model and natural halite systems.

2 Introduction

Extremely halophilic archaea are adapted to the highest possible salinity conditions, thriving in saturated brines. Microbial diversity in such environments is highly reduced and tends to be dominated by haloarchaea (Oren, 2006). Saturated brines are characterized by low dissolved oxygen content despite contact with the air and are often exposed to elevated temperatures and high levels of solar radiation (Oren, 2006; Merino *et al*., 2019) leading to evaporation. During evaporation events, the total contents of the brine, including salts, organics, some atmospheric gases, and any microorganisms present, are trapped within inclusions in the salt crystals. Viable halophilic bacteria and archaea have been isolated from halite (NaCl) of various ages, from months to years (Norton and Grant, 1988; Gramain *et al*., 2011; Huby *et al*., 2020), to geologically relevant timescales with the age of the primary halite given by the surrounding geological matrix. Some studies have even reported the observation or isolation of microorganisms from halite dated to several hundreds of millions of years (Vreeland *et al*., 2000; Schreder-Gomes *et al*., 2022). These observations have raised two important questions: (1) are these truly 'ancient' cells? (2) what physiological changes are required for microbial cells to remain viable within halite brine inclusions?

The first question has been studied in greater detail, and while many questions still remain, these studies provided valuable insights into the potential for surface-contaminant microorganisms (Graur and Pupko, 2001; Maughan *et al*., 2002; Nickle *et al*., 2002). In response to these criticisms, appropriate surface sterilization and cleaning procedures for microbial cultivation and DNA isolation for micro-biodiversity studies from dissolved ancient halite (Gramain *et al*., 2011; Sankaranarayanan *et al*., 2011) were developed. These approaches enabled more accurate identification of only those

microorganisms trapped within halite inclusions. Another opened question is whether the age determined from the geological context in which primary halite crystals were found can accurately be applied directly to the microorganisms in the brine inclusions. Dissolution and recrystallization of halite over geological time scales may contribute to the presence of more modern microorganisms (see discussion in Winters *et al.,* 2015 and references therein). No known microbial survival mechanism to date can account for cell viability over millions of years. Some studies have examined the possibility that microbial cell-like biomorphs are preserved within brine inclusions (Nims *et al*., 2021).

An alternative approach is to experimentally confirm how microbial life is supported within brine inclusions over durations known to support viable microorganisms. Determining the cellular functions expressed by viable halophiles within halite brine inclusions requires the direct isolation of biomolecules such as proteins and nucleic acids for "-omics" analyses, including proteomics and transcriptomics. However, significant technical challenges are presented by the closed system of brine inclusions within halite. Accessing the contents of brine inclusions by rapid crystal dissolution leads to cell lysis by osmotic shock and biomolecule degradation, while the time required for gradual crystal dissolution preserving cellular integrity is also sufficient for alterations in the transcriptomes and proteomes of viable cells away from their state within the brine inclusions. In addition, the direct extraction of biomolecules from brine inclusions involves a large amount of NaCl, which is incompatible with direct mass spectrometry analysis due to the lack of sufficient desalination steps in standard protocols. Although current hypotheses concerning the modifications of halophile physiology during entrapment within halite brine inclusions include a change to anaerobic metabolism (Winters *et al.,* 2015) along with potential for cell envelope modifications depending on conditions (Fendrihan *et al*. 2012; Kixmüller and Greie, 2012), these remain largely unverified at the molecular level due to these experimental challenges. New methods are needed to isolate proteins and RNA directly from halite brine inclusions, without allowing the microorganisms to alter their gene expression during salt dissolution and processing. The development of a new analytical workflow compatible with multi-omics analyses is best conducted with a known model organism for which there is a large repertoire of physiological studies and multi-omics data for liquid cultures exposed to a range of conditions applicable to halite brine inclusions (different oxygen availabilities, salinities, nutrient availabilities, etc.). For these reasons, we choose the model haloarchaeon *Halobacterium salinarum*, the type strain of the *Halobacteriales* family (Gruber, 2004; Oren, 2009).

H. salinarum is an appropriate model as it is found both in contemporary NaCl-saturated aqueous environments such as Great Salt Lake (Post, 1977) and has been detected in halite and closely related to isolates from ancient salt deposit (Mormile *et al*., 2003) The red pigmentation of *H. salinarum* strain is directly correlated with transmembrane proteins (bacteriorhodopsin and halorhodopsin) and carotenoids (bacterioruberin) also used by cells as antioxidants (Eichler, 2019). The accumulation of high intracellular concentrations of potassium (K^+) and chloride (Cl^-) (Engel and Catchpole, 2005), needed to maintain osmotic homeostasis, induces both biochemical adaptations (in the form of a strongly acidic proteome) as well as technical challenges to desalt cellular extracts. *H. salinarum* survives in changing environments by using a complex variable energetic metabolism with a preference for aerobic respiration but capable to switch under low oxygen conditions to phototrophy via bacteriorhodopsin, arginine fermentation or anaerobic respiration using dimethyl sulfoxide (DMSO) and trimethylamine oxide (TMAO) if available (Hartmann *et al*., 1980; Müller and DasSarma, 2005; Falb *et al*., 2008; Gonzalez *et al*., 2009). Established multi-omics protocols for liquid cultures of *H. salinarum* have permitted analyses of the cellular responses to a broad range of environmental conditions, including variations in NaCl (Leuko *et al*., 2009), pH (Moran-Reyna and Coker, 2014), oxygen (Schmid *et al*., 2007), and temperature (Coker *et al*., 2007), all relevant to halite brine inclusions. This existing knowledge base far exceeds that developed to date for halophiles isolated directly from ancient halite.

Here we present an efficient new analytical method for the study of microorganisms within halite, validated using *H. salinarum* entrapped in laboratory-grown halite to probe the question of what physiological changes are required for microbial cells to remain viable within halite brine inclusions, focusing on the initial phase of halite entrapment. The developed workflow includes removal of not only surface-attached cells and nucleic acids but also proteins, with subsequent extraction and desalting of proteins directly from brine inclusions compatible with mass spectrometry analyses. Applying these methods, we determined the acclimation of *H. salinarum* cells to inclusions at molecular level within laboratory-grown halite by analyzing the differences in the expressed proteome prior to evaporation and two months after culture evaporation. Analyses focused on the characterization of cellular activity compared to stationary cells not trapped within halite, as well as the interactions of cells with halite brine inclusion environment.

3 Material and Methods

All reagents used were analytical grade and suitable for molecular biology.

3.1 Strain and Culture Conditions

Halobacterium salinarum strain NRC-1 (JCM 11081) was grown under oxic conditions in autoclaved complex medium (CM: 4.28 M NaCl, 81 mM $MgSO_4.7H_2O$, 27 mM KCl, 10 mM trisodium-citrate.$2H_2O$, 1 % (w/v) peptone Oxoïd® LP0034, pH adjusted to 7.4) following Oesterhelt and Stoeckenius (1974) at 37 °C, 180 rpm. Growth was monitored by spectrophotometry at 600 nm (OD_{600}). Cultures for crystallizations, proteins and RNA extractions were grown to stationary phase (OD_{600} = 1.0 to 1.6) to approximate the physiological condition of haloarchaea under natural conditions during evaporation.

3.2 Laboratory-Grown Halite

3.2.1 Internally Inoculated Halite

Modeling entombment of haloarchaea within halite was already done in laboratory by Norton and Grant (1988), Gramain *et al*. (2011) and Kixmüller and Greie (2012). In this study, laboratory-grown halite crystals were produced following a modified version of protocols of Fendrihan *et al.* (2012), by adding nutrients to their Tris-buffered NaCl solution (TN buffer; 100 mM Tris-HCl pH 7.4, 4.28 M NaCl) to simulate cell lysis and metabolite release from less extreme halophiles concomitant with increasing NaCl concentrations in the natural environment just prior to halite precipitation (Winters *et al.*, 2015). Briefly, *H. salinarum* cells in stationary growth phase were harvested by centrifugation at 7 500 x g, 10 min, 20 °C and the growth medium removed by washing with sterile TN buffer. Cells were then resuspended in sterile TNPA buffer (TN buffer with 1 % (w/v) Oxoïd® peptone LP0034 and 0.5 % (w/v) L-Arg HCl, adjusted pH 7.4) with a ratio of 10 mL TNPA buffer per 500 mg of cells (wet weight). A 20 mL volume of cell resuspension was evaporated in each sterile 90/14.3 mm Petri dish in a 37 °C with a 12 h:12 h light:dark photoperiod (66,75 µmol photons.m^{-2}.s^{-2}, verified by a Li-250A, Li-Cor Inc., Germany) to model natural brine-surfaces. Complete evaporation and drying of precipitated halite were obtained after ~22 days, followed by a further 60 days (two months) of incubation to study the early phase of *H. salinarum* entombment within halite brine inclusions.

3.2.2 Externally Inoculated Halite

To produce halite with *H. salinarum* cells localized exclusively at the halite surface, 20 mL of sterile TN buffer was first evaporated as described above until complete drying (~ 22 days). The resultant crystals were then collected aseptically using sterilized forceps and the surfaces of each crystal inoculated with 4.5×10^9 *H. salinarum* cells in stationary phase, applied as a highly concentrated cell

solution after centrifugation (7 500 x g, 10 min, room temperature, RT°C). Crystals were inoculated on the largest faces (designated here as 'top' and 'bottom', see Figure 2k) by first inoculating the 'top' face drop-by-drop and spreading out using a sterile inoculating loop. Halite were then dried overnight at 37 °C, followed by the 'bottom' face the next day with the same protocol.

3.3 Scanning Electron Microscopy (SEM)

Observations and analyses of halite crystals were performed by first attaching the crystals directly to aluminum supports with carbon tape followed by carbon thin coating. Observations were performed using a Zeiss Ultra 55 field emission gun scanning electron microscope (SEM-FEG) equipped with a Brucker Energy dispersive X-ray spectroscopy (EDX) QUANTAX detector. Secondary and backscattered electron images and EDX analyses and maps were obtained at 10 kV and a working distance of 7.5 mm.

3.4 In-Brine Cellular Viability Tests

To assess cell viability after halite inclusion, salt crystals were weighted to determine the appropriated NaCl concentration required for the complex medium to obtain a final concentration of 4.28 M after halite dissolution as previously described by Gramain *et al.* (2011). Halite and complex medium were then incubated at 37 °C, 180 rpm. After crystal dissolution, culture OD_{600} was measured and cell morphology was visually inspected by optical microscopy. Pigmented (red) cultures reaching a normal stationary phase culture ($OD_{600} > 1.0$) were classified as viable and cultures showing no increase in OD_{600} after 1 month ($OD_{600} < 0.1$) were classified as non-viable.

3.5 Halite Surface Cleaning (Removal of Cells and Proteins)

3.5.1 Cold Atmospheric Plasma Treatment

Cold atmospheric plasmas (*i.e.*, weakly ionized gases) were generated were generated using either a dielectric barrier device (DBD) or an atmospheric pressure plasma jet (APPJ). They were polarized to the high voltage using two types of electrical power supply: (1) an alternative current (AC) generator composed of a function generator (ELC, GF467AF) and a power amplifier (Crest Audio, CC5500) as well as (2) a pulse generator (RLC electronic Company, NanoGen1 model) coupled with a high voltage power supply (Spellman company, SLM 10 kV 1200W model). DBD and APPJ were supplied with different a carrier gas (helium or argon) with/without oxygen. Hence several plasma conditions were performed to produce active species (radicals, reactive oxygen species but also electrons and photons).

182 The Table 1 details the experimental plasma conditions that were investigated as well as the resulting
183 proteolysis to assess the efficiency of protein removal.

184 **3.5.2 Chemical Treatments**

185 Previous studies applied surface cleaning protocols developed for removal of cells and nucleic acids,
186 as detailed in Supplementary Table 1. To adapt these protocols for the removal of surface-bound
187 proteins, we modified the protocol of Sankaranarayanan *et al*. (2011) using shorter time for baths to
188 avoid dissolution of smaller laboratory-grown crystals. Briefly, crystals were incubated in successive
189 5 min baths: 4.00 - 4.99 % NaOCl (Honeywell Research Chemicals; avoiding commercial bleach
190 solutions that induced rapid and near-complete crystal dissolution) in saturated NaCl and 10 M NaOH
191 in saturated NaCl supplied or not with 10 N HCl followed by 100 mM Na_2CO_3 in saturated NaCl. A
192 sterile saturated NaCl was used to wash off each treatment solution between each successive bath,
193 testing both passive wash baths and active-spray washes using a hemolytic pump.

194 **3.6 Protein Extraction and Preliminary Desalting**

195 All solvents used for protein extractions were HPLC-grade and suitable for mass spectrometry analysis.
196 Extractions were performed with TRIzol Reagent™, based on the halophilic protein extraction protocol
197 of Kirkland, *et al*. (2006). This protocol was modified for protein extraction directly from halite crystals
198 with high salt content and proteomics analysis by mass spectrometry. Compatibility for liquid cultures
199 was kept as described below. All steps described were performed with autoclaved glassware to avoid
200 any organics contamination from plastics (bench top protocol see Supplementary Section 2). Crystals
201 were fully immersed in 5 mL of TRIzol Reagent™ in 30 mL glass centrifuge tube and crushed using
202 autoclaved glass stir-rod. After 20 min incubation at 60 °C, total RNA was extracted from the resulting
203 cell lysate by adding 1 mL of 100 % chloroform, incubating for 5 min at room temperature followed
204 by phase separation by centrifugation (10 000 x g, 20 min, 4 °C). The chloroform-containing aqueous
205 phase was removed with autoclaved glass Pasteur pipet and 1.5 mL of 100 % ethanol was added to
206 precipitate DNA. After 3 min at room temperature, supernatant was collected by centrifugation (2 000
207 x g, 10 min, 4 °C). Proteins were precipitated with 7.5 mL of 100 % isopropanol and collected by
208 centrifugation (10 000 x g, 20 min, 4 °C). The resulting protein pellet was washed twice to remove
209 phenol traces using 5 mL of 0.3 M guanidine-HCl in 95 % ethanol to denature the proteins, followed
210 by a third wash step with 5 mL of 100 % ethanol to remove any residual guanidine-HCl. Each wash
211 step was performed by incubating the cell pellet in the solution for 20 min at room temperature followed
212 by centrifugation (10 000 x g, 20 min, 4 °C). Protein desalting was accomplished by two successive

213 protein precipitations with 2 mL of 100 % glacial acetone (-20 °C) and centrifugation (10 000 x g, 20
214 min, 4 °C). After acetone removal, the pellet was completely dried under laminar flow. Proteins were
215 then solubilized in 1 M $NaHCO_3$ with 0.1 % SDS at room temperature for two days and quantified
216 with a bicinchoninic acid (BCA) proteins assay (Pierce) using either bovine serum albumin (BSA)
217 standards concentration from manufacturer's instruction for quantitative mass spectrometry or adapted
218 BSA standard concentrations for low protein concentrations (see Supplementary Information, Section
219 3) for evaluating removal of halite surface-bound proteins. Proteolysis rate was determined by proteins
220 quantity comparison with and without treatments.

221 Total proteins were extracted from *H. salinarum* cultures in stationary growth stage using a
222 similar procedure. For this, 2.0 x10^{10} cells from liquid cultures were pelleted by centrifugation (7 500
223 x g, 10 min, 20 °C) and the cell pellets directly resuspended in 5 mL TRIzol Reagent™ solution, prior
224 to following all steps described above for halite samples. After solubilization of the protein pellet,
225 solubilization with 1M $NaHCO_3$ with 0.1 % SDS at room temperature, protein quantification was
226 performed using the BCA assay (Pierce) protein assays as per the manufacturer's instructions.

227 **3.7 iTRAQ® Isobaric Labelling and Mass Spectrometry**

228 Aliquots of 100 µg of proteins for each sample condition and replicate were reduced using 2 mM of
229 tris-(2-carboxyethyl) phosphine (TCEP) at 37 °C for 1 h, and alkylated with 5 mM of iodoacetamide
230 30 min in the dark at RT°C prior to digestion with 5 µg of trypsin Gold (Promega) for 15 h at 37 °C.
231 After digestion, additional desalting of peptides was done directly by solid phase extraction (SPE)
232 using C18 cartridges (Sep-Pak C18 Plus Short 400 mg Sorbent, Waters). The resulting peptides were
233 dried by speed-vac and resuspended in tetraethylammonium bromide (TEAB) 0.5 M prior to labelling.
234 iTRAQ® labelling was performed according manufacturer's instructions (Applied Biosystems).
235 Briefly, each of the iTRAQ® isobaric labelling reagents were reconstituted with isopropanol and then
236 added to the 50 µg of protein digest (113, 114, 115 and 116 iTRAQ® isobaric labels for proteins from
237 liquid controls and 117, 118, 119 and 121 for halite brine inclusions protein extractions). After 2 h at
238 room temperature, samples were desalted again with C18 SPE. The labelled peptides eluted were then
239 dried by speed-vac and resuspended in 2 % acetonitrile, 98 % H_2O with 0.1 % formic acid (see
240 Supplementary Information, Section 4 for additional details).

241 Labelled peptide samples were analyzed by mass spectrometry as previously described (Pinel-
242 Cabello *et al.,* 2021) on a Q Exactive HF tandem mass spectrometer (Thermo Scientific) coupled to an

243 UltiMate 3000 Nano LC System. Peptides were desalted online on an AcclaimPepmap100 C18
244 precolumn (5µm, 100 Å, 300 µm i.d x 5 mm) and further resolved on a nanoscale AcclaimPepmap100
245 C18 column (3 µm, 100 Å, 75 µm i.d. x 500 mm) at a flow rate of 200 nL min^{-1} using a 120-min
246 gradient of 4-32 % acetonitrile. A Top 20 strategy was applied in data dependent acquisition mode.
247 Full scan mass spectra were acquired from 350 to 1800 *m/z* at a resolution of 60,000 with an automatic
248 gain control (AGC) target set at 3×10^6 ions. MS/MS fragmentation was initiated when the ACG target
249 reached 10^5 ions with an intensity threshold of 9×10^4. Only precursor ions with potential charge states
250 of 2^+ and 3^+ were selected for fragmentation applying a dynamic exclusion time of 10 s.

251 **3.8 Mass Spectrometry Data Analyses**

252 **3.8.1 Protein Identification**

253 Protein identifications were performed using PEAKS® X-Pro software (64 bits version, 2020,
254 BioInformatics solutions). It allows database search assisted *de novo* sequencing against the protein
255 coding sequences from *H. salinarum* NRC-1 (8 533 entries from NCBI, download date 2021/08/03).
256 Spectral peptides matching was carried out with the following parameters: (1) mass tolerance of 10
257 ppm on the parent ion, (2) mass tolerance of 0.005 Da for fragment ions from MS/MS, (3)
258 carbamidomethylated Cys (+57.0215) and iTRAQ® isobaric tag Lys and N-terminal (+304.2054) as
259 fixed modifications; and (4) oxidized Met (+15.9949), deamidated Asn and Gln (+0.9840) and
260 iTRAQ® isobaric tag Tyr (+304.2054) as variable modification. The false discovery rate (FDR) was
261 estimated with decoy-fusion option included in the software. Proteins were then filtered with FDR < 1
262 % (corresponding to a -10logP score above 25) for peptide-spectrum matches (PSMs) and a valid
263 protein identification required minimum 2 unique peptides with a -10logP score above the peptide
264 filtering threshold that can be mapped to only one protein group.

265 **3.8.2 Protein iTRAQ® Quantitation**

266 The eight labelled samples (four replicates each of proteins from liquid stationary cultures and from
267 halite brine inclusions) were mixed in equimolar ratios and injected in nanoLC-MS/MS in triplicate to
268 reduce instrument variability as previously described. Quantitation was performed using PEAKS Q
269 (quantitation program) iTRAQ 8-plex type with 10 ppm mass tolerance and only peptides with a score
270 above FDR threshold 1 % are used to quantify the identified proteins. Resulted quantitation was filtered
271 accepting only proteins groups with fold change ≥ 2, at least two unique peptides and FDR adjusted ≤
272 1 % for both proteins identification and fold change significance using ANOVA significance method.

Mass spectrometry proteomics data have been deposited to the ProteomeXchange Consortium via the PRIDE partner repository with the dataset identifier PXD037167 (project DOI: 10.6019/PXD037167).

3.8.3 Sample Comparisons and Functional Annotation

Potential biases during analysis were avoided by filtering protein identifications produced using the PEAKS software to group proteins having multiple annotations in the NCBI database. To do so, we developed custom BASH and PYTHON scripts to merge all descriptions for one proteins identifier (favoring in order AAG-type, DAC-type, WP-type and then Q9H-type identifier). Venn diagrams were computed with VennDiagram and ggplot2 packages in R script. Functional proteins annotation was done with Kyoto Encyclopaedia of Genes and Genomes (KEGG, Kanehisa and Goto, 2000) using blastKOALA tool (Kanehisa *et al*., 2016; https://www.kegg.jp/blastkoala/), assigning K numbers to identified proteins (see Supplementary Table 6-2). K number were then used for mapping identified proteins onto pre-existing metabolic pathways using KEGG Mapper search tools (https://www.kegg.jp/kegg/mapper/search.html ; see Supplementary Table 6-3).

3.9 Total RNA extraction and analysis

Total RNA for transcriptomics analyses were extracted using TRIzol Reagent™ method described above for protein extractions with the following modifications. To avoid RNA degradation, the TRIzol Reagent™ mixture with pulverized halite crystals was incubated for 5 min at room temperature rather than 20 min at 65 °C as recommended by the manufacturer. The chloroform phase was then collected by centrifugation and RNA purification was perform using RNeasy MinElute cleanup columns (Qiagen). Resulting RNA were quantified using QuBit Q32857 (Invitrogen) the purity assayed using Nanodrop 2000/2000c (Thermo Scientific), and the quality was determined with the BioAnalyzer 2100 system (Agilent). All steps after RNA extraction were performed according manufacturer's instructions with RNAase-free materials and solutions.

4 Results

4.1 Characterization of Laboratory-Grown Halite Containing *H. salinarum*

In order to study the physiology of *H. salinarum* cells after entombment within brine inclusions, we first needed to characterize the laboratory-grown halite, including resultant crystal size, cell localization, and surface-bound biomolecules. This enabled the establishment of selection criteria for downstream proteomics analyses and the development of protocols to exclude any 'contaminant' proteins from the surface of the crystal.

4.1.1 Variability of *H. salinarum* cells from Inoculated Laboratory-Grown Halite

Laboratory-grown halite crystals produced from TNPA solutions containing *H. salinarum* cells using a slow evaporative process exhibited heterogeneous crystallization with respect to crystal size and coloration. As shown in Figure 1, even replicates produced under the same conditions produced different quantities of crystals of varying lengths and widths, but with relatively uniform thicknesses (±1 mm) of hopper and fishtail crystals. Color variations observed for halite in this study were likely the result of heterogeneities in the number of brine inclusions containing pigmented *Halobacterium* cells. The red color indicative of *H. salinarum* cells tended to concentrate in the center of hopper crystals where inclusions were most abundant (Roedder *et al*., 1984). Individual crystals of similar size and coloration were collected aseptically for further study, selecting only halite without visible defects signaling potential rupture of near-surface brine inclusions.

4.1.2 Contaminating Surface-Bound Cells and Proteins

To evaluate the potential for 'contaminating' microbial cells or residual biomolecules at the crystal surface, the elemental composition of halite with and without *H. salinarum* cells were determined by SEM-EDX. Elemental analyses of control halite derived from evaporation of the TNPA solution only exhibited the expected sodium chloride crystal surface, along with dense, irregular C agglomerates (Figure 2c-f) derived from the presence of organics (peptone, L-Arg) in the TNPA solution. The addition of *H. salinarum* cells to the TNPA solution prior to evaporation produced similar structures to control crystals, with no intact cells of *H. salinarum* visible on halite surfaces (Figure 2i,j). However, EDX analyses revealed differences in the distribution of carbon compared to control samples, as well as the presence of microscopic KCl crystals at the halite surface (Figure 2j) that were not found on control TNPA-derived crystals without *H. salinarum* cells. These differences were likely due to lysis of surface adhered *H. salinarum* cells releasing high concentration of cytosolic K^+ and Cl^- accumulated as part of the "salt-in" osmoadaptation strategy (Engel and Catchpole, 2005). In order to assess both the potential for surface bound contaminants, including viable cells as well as proteins, externally inoculated halite were produced (Figure 2k). After these externally inoculated halite crystals were dissolved in growth medium and incubated at 37 ˚C, 180 rpm. Such cultures reached a normal stationary phase culture ($OD_{600} > 1.0$), demonstrating that at least a sub-population of halite surface-attached cells were viable. observations of these cultures showed rod-shaped cells with low motility. Additionally, SEM-EDX analysis of externally inoculated crystals revealed a similar elemental composition and distribution to that of internally inoculated halite (bearing cells both within brine inclusions as well as on the halite surface) after two months post-evaporation (Figure 2m,n). Taken

together, these results confirm the presence of both viable cells and cellular debris on the surface of halite after two months of desiccation, validating the need for halite surface cleaning procedure to remove any residual proteins.

4.2 Development of Total Protein Isolation Methods for Halite

For proteomics approaches inside crystals without prior dissolutions, a new methodology for direct proteins extraction from brine inclusions was developed. This method was based on the protocol of Kirkland *et al*. (2006) for liquid cultures to allow mass spectrometry analysis compatible both for crystals and liquid cultures with TRIzol Reagent™ (see Supplementary Information, Section 4 for details on the parameters tested during protocol development and optimization). Briefly, protocol was modified to optimize desalting steps (due to direct halite extraction with high NaCl content), protein pellet dissolution and protein digestion.

4.3 Development of Proteolysis Protocols for Removal of Halite Surface-Bound Contaminants

Previous halite cleaning procedures from Gramain *et al*. (2011) and Sankaranarayanan *et al*. (2011) (see Supplementary Table 1) were developed to deactivate surface-contaminating microorganisms and remove surface-contaminating DNA. However, these methods were not designed for the removal of other types of biomolecule contaminants, such as proteins. A new, modified surface cleaning procedure was therefore needed to remove surface protein contamination to enable extraction of proteins only from within halite brine inclusions while avoiding crystal dissolution during the cleaning process. To meet these requirements, both cold plasma treatments and chemical protocols were tested using externally inoculated halite.

Cold plasma exposure is routinely used in astrobiology to sterilize spacecraft surfaces of microbial contaminants prior to launch. For this reason, a cold plasma approach was investigated here for the decontamination of halite surface. Two plasma sources – a DBD and an APPJ – were tested as an alternative to conventional liquid solvents. The expected benefit was to minimize halite dissolution-recrystallization events, hence ensuring the survival of the microorganisms within the halite. However, owing to their insulating properties and irregular topography, halite crystals attenuate plasma electric field and/or bend its field lines. As a result, and whatever the implemented plasma treatment (Ar, He, He mixed with O_2), the externally inoculated halite crystals still retained the pink coloration which is indicative of the protein and lipid pigments of *H. salinarum* cells (data not shown). As shown in Table 1, the most efficient plasma treatment drove to partial cell lysis (as determined by culture-based viability tests following growth by OD_{600}) and to a proteolysis of only 39.1 % based on extraction and

366 quantification of remaining proteins from halite surfaces using a modified BCA assay for low protein
367 quantities; a value that remains insufficient for the application.

368 As an alternative, chemical treatments were tested, using protocols modified from the
369 microorganism deactivation and DNA removal treatments of Sankaranarayanan *et al*. (2011) to extend
370 to proteolysis. First, reduction of the exposure times in each chemical bath from previously published
371 protocols were tested to avoid crystal dissolution, while maintaining the use of NaCl-saturated
372 chemical solutions to avoid crystal dissolution. Subsequent, 5-minute sequential NaOCl and NaOH
373 treatments, either with or without additional HCl treatments, resulted in insufficient halite surface
374 proteolysis (Supplementary Figure 5-1a). This was likely due to the rough structure of hopper crystals,
375 which could allow proteins to remain attached during passive chemical baths. After chemical
376 treatments partially degraded the contaminating biomolecules and reduced their attachment to the halite
377 surface, an active-spray method was used for wash steps to increase the efficiency of biomolecule
378 removal and prevent re-association with halite surfaces, compared to the use of passive wash baths
379 (Supplementary Figure 5-1b). This active-spray method also allowed for both deactivation of halite
380 surface-bound microorganisms (as indicated by a lack of culture growth in post-treatment viability
381 tests) and better protein lysis compared to passive chemical bath washes. Using the protein extraction
382 method described above, the efficacy of active-spray method for removal of surface-bound proteins
383 was tested comparing NaOCl-NaOH and NaOCl-NaOH-HCl protocols. A shown in Figure 3a, addition
384 of an acid wash results in a proteolysis efficiency of 93.0 ± 4.3 %, compared to from of 83.7 ± 15.9 %
385 without the HCl treatment step (residual proteins 51.6 ± 31.6 µg and 120.5 ± 117.6 µg, respectively,
386 n=3). These results suggest that NaOCl-NaOH-HCl active-spray washes protocol (Figure 3b) present
387 optimal and more consistent surface proteolysis, particularly for the small laboratory-grown halite
388 crystals used in this study.

389 To ensure that this active-spray chemical treatment did not affect *H. salinarum* cells within the
390 halite brine inclusions, growth was monitored for crystals containing cells trapped in brine inclusions
391 after surface chemical cleaning with active-spray NaOCl-NaOH-HCl treatment. Viable cultures were
392 obtained from dissolution of the crystals in CM growth medium, thereby validating the active-spray
393 chemical surface protein removal protocol for use in studying biomolecules within halite brine
394 inclusions.

395 These new methods for removal of surface-bound proteins followed by extraction of total
396 proteins from halite brine inclusions using a modified TRIzol Reagent™ method with desalting were

397 then applied to answer the question of how *H. salinarum* acclimates to halite brine inclusions over the
398 initial phase post-evaporation using proteomics

399 **4.4 Proteomic Shifts in *H. salinarum* Induced by Acclimation to Halite Brine Inclusions**

400 Total proteins were extracted from the brine inclusions of halite after two months of complete dryness,
401 with surface-bound proteins removed using the new protocol detailed above. These brine inclusions
402 extracts were compared to total proteins extracted from *H. salinarum* cultures in stationary growth
403 phase, representing conditions prior to halite formation. The proteins unique to each condition, as well
404 as the common proteome between liquid cultures and from halite interiors were analyzed to determine
405 how *H. salinarum* acclimates to halite brine inclusions.

406 Using the mass spectrometry data of four replicates from each condition, 1 249 total proteins
407 were identified from stationary phase liquid cultures and 1 052 from halite brine inclusions,
408 representing 1 342 unique proteins. Comparisons of the four replicate samples per condition revealed
409 a core proteome composed of 839 proteins common to all sample replicates for liquid cultures and 715
410 proteins for halite brine inclusions extracts (Figure 4 a, b). Of these, 655 proteins were expressed by
411 cells both in liquid cultures and within halite brine inclusions (hereafter referred to as "shared
412 proteins"); while 60 were specific to halite brine inclusions samples and another 184 were only
413 identified from liquid cultures (Figure 4c, Supplementary Table 6-1). KEGG blastKOALA searches
414 provided matches for roughly 75 % of these shared proteins (488 of 655 shared proteins), as well as 62
415 % of proteins unique to halite brine inclusions samples (37 of 60 proteins) and 52 % of proteins unique
416 to liquid cultures (95 of 184 proteins) (see Supplementary Table 6-2), allowing for functional pathway
417 reconstruction. The halite brine inclusions proteome contained genome maintenance and repair
418 proteins (Nth, UvrB, MutS2) not found expressed by cells from liquid cultures, along with multiple
419 enzymes implicated in amino acid metabolism, metabolism of cofactors, and membrane transport (see
420 Figure 6 and Supplementary Table 6-3).

421 As a qualitative approach is insufficient to determine the regulation of proteins leading to their
422 differential expression for *H. salinarum* cells within halite brine inclusions, a semi-quantitative mass
423 spectrometry analysis was also performed. Results from all three injections were pooled to reduce
424 instrument variability (Figure 5). Subsequently 68 proteins from halite brine inclusions were identified
425 with statistically significant changes in expression levels compared to liquid cultures (fold change ≥ 2;
426 see Supplementary Table 6-4 and Supplementary Figure 6-1). KEGG blastKOALA searches provided
427 functional pathway results for 80 % of down-regulated proteins (35 of 44 proteins) and 71 % of up-

428 regulated proteins (17 of 24 proteins) (see Supplementary Table 6-2). Up-regulated proteins included
429 metal transporters, redox reactions, acetyl-CoA production, and the UgpB glycerol-3-phosphate-
430 binding protein precursor. Down-regulated proteins were predominantly ribosomal subunits, indicating
431 reduced translational activity (see Figure 6 and Supplementary Table 6-3). To determine whether there
432 was a corresponding downwards shift in transcriptional activity for cells inside halite brine inclusions
433 compared to liquid cultures, RNA extractions were performed.

434 4.5 Reduced Total RNA Concentration Within Halite Brine Inclusions

435 The advantage of a TRIzol Reagent™-based extraction method is that it allows for extraction of not
436 only proteins, but also nucleic acids (DNA, RNA), and lipids (Podechard *et al.,* 2018) for complete
437 multi-omics analyses. To this end, the new methodology presented here was applied to extract and
438 purify RNA from surface cleaned, internally inoculated halite after two months of incubation at 37 ˚C
439 to complement the proteomic analyses. Consistent with the reduced quantities of ribosomal proteins
440 observed for halite brine inclusions extracts, low quantities of RNA were obtained from brine extracts
441 compared to stationary cells extracts (Table 2). In addition, the quality and purity of the resultant RNA
442 from halite was lower than that from liquid cultures (Supplementary Figure 6-2). To determine if this
443 low-quality RNA was due to the age of the samples (two months after drying) or degrading effects of
444 halite salts on RNA during extraction, extractions of RNA were performed from fresh externally
445 inoculated halite (*i.e.*, approximatively one week after external cells addition) using the same protocol.
446 RNA extractions from these 'young' crystals presented higher quantity and purity compared to those
447 from halite brine inclusions after two months, but still lower quality and purity than RNA extracted
448 from liquid cultures.

449 5 Discussion

450 The initial objective of this study was to determine the molecular acclimation of haloarchaea to
451 entrapment within halite brine inclusions using a proteomics approach. To this aim, we first needed to
452 (1) better characterize the process of laboratory-based evaporation for halite entrapment of haloarchaea
453 and its effects on both the resulting halite and the microbial cells, (2) develop efficient methods for the
454 removal of halite surface-bound cells and biomolecules in order to isolate only proteins contained
455 within the brine inclusions, (3) develop effective methods for protein extraction directly from halite
456 brine inclusions in a shorter time period to avoid alterations in protein expression that can occur during
457 gradual salt dissolution, and finally (4) combine these approaches to analyze total proteins and RNA
458 from *H. salinarum* extracted from halite brine inclusions and compare these to control samples from

stationary phase liquid cultures in order to propose a model of acclimation within halite. A slow evaporative process was chosen to generate the internally inoculated halite to model natural processes that occur over time scales sufficient for cellular acclimation to the environmental changes, rather than a rapid "shock" evaporative process.

5.1 Biotic/Abiotic Interactions Influencing Halite Formation and *H. salinarum* Viability

Similar to previous studies of survival of halophiles within halite brine inclusions, a NaCl-based buffered evaporation solution was used in this study (Norton and Grand, 1988; Fendrihan *et al*., 2012; Kixmüller and Greie, 2012). However, here we chose to add nutrient sources (1 % peptone, 0.5 % L-Arg HCl) to simulate organics present in the natural environment. This enabled us to study the role of metabolism in the survival and acclimation processes of *H. salinarum* cells to the early phases of entrapment within halite brine inclusions. The presence of microbial biomass and additional organics can affect halite precipitation processes and also explain the observed crystallization heterogeneity observed. For example, Norton and Grant (1988) previously demonstrated a positive correlation between the initial microbial cell density in liquid culture and the quantity of halite brine inclusions formed during evaporation.

The presence of nutrients seemed to diminish rather than increase the duration of survival. While Gramain *et al*. (2011) observed growth of *H. salinarum* NRC-1 after 27 months post-entombed in halite, there were some notable differences in the experimental parameters used. Gramain *et al*. (2011) used evaporation buffers with different compositions of nutrients to the evaporation buffer (either without nutrients or with addition of 0.01 % Difco yeast extract and 0.0075 % Merck casein hydrolysate diluted from the standard concentrations in modified Payne's medium of 1 % and 0.75 %, respectively, Payne *et al.,* 1960), incubated the resulting salt crystals in the dark at room temperature rather than with a 12 h:12 h diurnal cycle at 37 ˚C as used here, and did not appear to employ halite surface sterilization or cleaning protocols prior to these survival tests. In contrast, our viability tests of *H. salinarum* cells from internally inoculated crystals incubated at 37 ˚C over 80 days prior to subjected to surface organics cleaning treatments, dissolution and culturing showed no growth. The lower duration of survival observed for *H. salinarum* cells inside halite in our study may be the result of increased metabolic activity due to the higher concentration of nutrients in TNPA solution compared to the 100-time diluted modified Payne's medium used in Gramain *et al*. (2011). This could result in an inhibitory effect due to the accumulation of toxic waste products within the closed microenvironment of halite brine inclusions. The products of arginine fermentation include ornithine,

CO_2 and NH_4^+. While the addition of peptone in this present study provided sufficient trace elements (Mg^{2+}, K^+, etc.) for nominal cell functions and S-layer stability at the moment of halite formation, these nutrients may be depleted over time within the closed environment of brine inclusions (Kixmüller and Greie, 2012), concurrent with the buildup of waste products. In contrast, Winters *et al.* (2015) showed that starvation of *H. salinarum* leads to smaller cell size, and hypothesized that this condition could contribute to extended survival within halite brine inclusions. This is somewhat counter-intuitive as natural evaporite environments contain the lysed remains of dead cells and other sources of organics.

On the other hand, in the absence of surface sterilization of halite used in the viability studies in Gramain *et al.* (2011), some of the surviving cells observed in the study may have been the result of surface-adhered cells rather than cells within the halite brine inclusions. These results also suggest a possible survival advantage for cells on halite surfaces rather than those within the brine inclusions over the early stages of evaporation and acclimation, a hypothesis supported by the findings of Gramain *et al.* (2011) showing no difference in growth for *H. salinarum* cells evaporated in salt buffer without nutrients and those containing the diluted Payne's medium nutrients. This epilithic lifestyle is likely supported in part by the organics, K, and Cl observed in this study by SEM-EDX analyses to accumulate on the halite surface, derived from the lysis of *H. salinarum* cells. It is important to note that the vacuum conditions for SEM observations may have resulted in rupture of unfixed *H. salinarum* cells, which may have otherwise remained intact under normal atmospheric conditions.

Altogether, these results of surface contamination confirm that the isolation of proteins exclusively from halite brine requires the removal of halite surface-bound cells and biomolecules.

5.2 Removal of Halite Surface-Bound Microorganisms and Biomolecules

The small sizes of laboratory-grown halite proscribe the use of treatment processes that could result in salt dissolution. Cold atmospheric plasmas were therefore tested in an effort to avoid the use of liquid cleaners based on their effectiveness for the sterilization of spacecraft surfaces for planetary protection (Shimizu *et al*., 2013) and agricultural applications (Judée *et al*., 2021). Unfortunately, none of the plasma conditions tested in this study (gas mixtures, power delivery modalities) enabled a complete removal of proteins from the rough textured halite surfaces. However, the results remain encouraging insofar as cold plasma has demonstrated some effects on proteolysis that must now be amplified. Further experiments will be required to innovate an *ad hoc* plasma process delivering active species at higher densities while treating the whole surface of halite regardless their roughness surface, dimensions or dielectric permittivity.

The deactivation of microorganisms and removal of nucleic acids from halite surfaces were been therefore instead performed by adapting chemical wash methods first developed by Rosenzweig *et al*. (2000) and then optimized by Gramain *et al*. (2011) and Sankaranarayanan *et al*. (2011). By reducing the exposure times in sequential NaOCl, NaOH, and HCl treatments, and replacing passive chemical baths with an active spray process, we were able to achieve sufficient proteolysis of surface-bound proteins for downstream isolation of proteins exclusively from within halite brine inclusions, while avoiding halite dissolution during treatment. Compared to total proteins extracted from surface sterilized internally inoculated crystals (± 1 mg order), residual surface bound proteins (51.6 µg) were marginal. However, observations of residual pigmentation after removal of halite surface-bound proteins suggests the presence of non-protein pigments such as carotenoids. Further refinements are therefore needed before future studies can isolate lipids exclusively from within halite brine inclusions.

5.3 Limitations of the TRIzol Reagent™ Based Method for Direct Extraction of Biomolecules from Halite Brine Inclusions

TRIzol Reagent™ has the distinct benefit of enabling selective extraction of proteins, lipids, and nucleic acids. While TRIzol-based protein extraction methods have previously been used and validated to study proteins from liquid cultures of haloarchaea (Kirkland *et al*., 2006; Bidle *et al*., 2008). This study employed modified procedure that allow direct proteins extraction from salts crystals and subsequent desalinations steps were developed specifically for proteomics analysis from these high salt extracts. The results obtained after modifications of the procedure by Kirkland *et al*. (2006) appear compatible and efficient for semi-quantitative mass spectrometry approach directly on halite brine inclusions. Most importantly, our approach avoids induced bias in proteome due to alterations in protein expression over the extended times needed for a slow crystal dissolution prior to protein extraction using other methods.

Although peripheral membrane proteins were identified using this approach, transmembrane peptides were absent in the mass spectrometry dataset. We hypothesize that this was due to retention of transmembrane protein domains with the lipid membrane fraction during TRIzol Reagent™ extraction in residual phenol phase after protein precipitation with isopropanol. Importantly, some transmembrane proteins could be identified by peptides outside the membrane-spanning domains *e.g.*, the ArcD arginine-ornithine antiporter protein, for which seven cytosolic- and extracellular-facing peptides were identified (see Supplementary Figure 7-1). However, not all transmembrane proteins were identified as evidenced by the lack of identified peptides for bacteriorhodopsin in any samples

(stationary phase liquid cultures and brine inclusions). One plausible explanation of this phenomenon is the desalting effect of isopropanol (as suggested by Kirkland *et al*., 2006) that can result in increased protein instability, leading to loss of conformation and subsequent peptide fragmentation for peptides outside the transmembrane regions. While these results indicate that further membrane disruption steps may be needed for complete extraction of all transmembrane proteins, similar to the protocol used by Podechard *et al*. (2018) to isolate membrane lipids using TRIzol, the potential bias introduced by our methodology is limited, as evidenced by the identified peptides on either side of the lipid membrane.

While the low quantities of RNA extracted from halite brine inclusions were likely the result of low transcriptional activity based on the down regulation of ribosomal proteins observed during proteomics analyses (see following section), it might also be due to degradation of RNA over time within the brine inclusions. RNA quantity, purity and quality were insufficient to allow transcriptomic analyses for brine extracts (see Table 2). The quantity, quality and purity scores for fresh externally inoculated crystals were higher than those for surface sterilized crystals incubated for two months. Further desalting steps may help to improve future RNA extraction directly from halite.

5.4 Cellular Origin of Total Brine Extracted Proteome

The proteins extracted using the protocol presented here represent the total protein complement of the halite brine inclusions. These proteins may be components of viable or non-viable cells, or even proteins released by cells into the extracellular environment of the brine inclusions. Many questions remain about the potential for salts to preserve proteins over time as molecular biosignatures, particularly within the protected evaporite brine inclusions microenvironment. However, as the *H. salinarum* cells studied here remained viable during the two months of this study, we can hypothesize a cellular origin for the extracted proteins.

5.5 Acclimation of *H. salinarum* to Halite Brine Inclusions

We applied the slow laboratory evaporation method to *H. salinarum* cultures in TNPA buffer followed by removal of halite surface-bound cells and organics (particularly proteins) and selective extraction of proteins from within halite brine inclusions described in the preceding sections. This allowed us to study the early (two month) acclimation of the haloarchaeal cells to halite brine inclusions using a proteomics approach. Stationary growth phase cultures were used as a control to approximate the cell physiology prior to a slow evaporative process. Our analyses were focused on two main themes: (1) cell activity, and (2) interactions between cells and local microenvironment within the brine inclusion.

The investigations of the cell activity targeted proteins involved in central metabolism, energy production, cell division, replication, transcription and translation pathways. The cell interactions with the closed halite brine inclusions microenvironment were examined via cell envelope proteins (surface layer cell wall proteins and transporters) as well as proteins involved in the motility processes (chemotaxis, gas vesicle and archaellum).

5.5.1 Cell Activities Within Halite Brine Inclusions

A summary of the proteomics results is shown in Figure 6, showing shared proteins between cells from the stationary growth phase cultures and brine extracts as well proteins differentially expressed (up- or down-regulated) in halite-derived samples. Among the shared proteome showing no differential expression between conditions were proteins involved in DNA replication, reparation and transcriptional pathways. This suggests similar levels of genome maintenance between late growth stage cultures and brine entombment. However, translational proteins were not detected in brine extracts, potentially indicating decreased *de novo* protein synthesis compared to stationary cells. These seemingly contradictory results can be explained by transcriptional activity directed not to mRNA synthesis but to regulatory RNA. However, this hypothesis is not fully satisfactory as tRNA synthesis and ribosomal biogenesis protein quantities remain similar for both conditions.

5.5.1.1 Retention of Proteins for Central Metabolism

Proteins involved in central metabolism, including key enzymes involved in glycolysis/gluconeogenesis and the TCA cycle, formed part of the shared proteome between halite brine inclusions extracts and stationary phase liquid cultures (Figure 6). Additionally, proteins involved in arginine fermentation and aerobic respiration were shared between halite brine inclusions and stationary growth phase liquid cultures. The microenvironment of halite brine inclusions is assumed to be oxygen poor due to the combination of low oxygen diffusivity at high salinities as well as the closed microenvironment of brine inclusions. The metabolism of *Halobacterium* cells trapped within such inclusions is therefore hypothesized to shift from aerobic metabolism by respiratory chain to anaerobic fermentation or phototrophy through arginine deiminase pathway (ADI). Halite incubations were performed in this study with a 12 h:12 h light:dark photoperiod, allowing for both phototrophy via bacteriorhodopsin (ATP generation by photophosphorylation) and arginine fermentation (ATP generation by substrate-level phosphorylation) under oxygen-limited conditions (Hartmann *et al.*, 1980), as are presumed to exist inside closed brine inclusions. These two ATP-generating pathways are antagonistic for liquid cultures of *H. salinarum*, but can theoretically alternate over the diurnal

613 cycle used here to simulate surface conditions 2 months after halite precipitation. While the extraction
614 protocol used enabled identification of phototrophy-related proteins such as bacteriorhodopsin
615 activators, it did not allow for extraction of many membrane proteins including bacteriorhodopsin
616 itself. Thus, it is not possible to determine if phototrophy-related proteins were differentially expressed
617 in liquid and halite samples. Under anaerobic conditions, Hartmann *et al.* (1980) showed that while
618 retinal biosynthesis was inhibited by the absence of oxygen, even low levels of bacteriorhodopsin could
619 produce appreciable levels of ATP. A basal expression of proteins for different ATP generating
620 pathways could enable the survival of *H. salinarum* in the early stages of halite entombment. The
621 reduced viability of *H. salinarum* in brine inclusions in the presence of organics including arginine
622 compared to starvation conditions seems to favor fermentative metabolism leading to the accumulation
623 of potentially toxic waste products.

624 Quantitative analyses showed that the majority of proteins involved in pyruvate metabolism
625 maintained consistent expression levels after two months of halite inclusion with the exception of up-
626 regulation of proteins involved in acetyl-CoA production. Surprisingly, transporters and enzymes
627 involved in ADI pathway were expressed by both cells in stationary phase liquid cultures and brine
628 inclusions extracts, including the arginine deiminase, ornithine-carbamoyl transferase, carbamate
629 kinase, arginosuccinase, arginosuccinate synthetase, arginine-ornithine antiporter and an IclR family
630 transcriptional regulator. Only arginine deaminase was found significantly up-regulated for cells from
631 halite brine inclusions. Proteins for key components of the electron transport chain, including NADH
632 dehydrogenase/oxidoreductase subunits B, C, D and I, NAD(P)/FAD-dependent oxidoreductase,
633 succinate dehydrogenases and ATP synthase subunits A, B, C, D, E, H and I were not found to be
634 differentially regulated between cells from free-living (liquid cultures) or trapped within halite brine
635 inclusions (with the exception of with F subunit lacked in one brine inclusions extract). Confirmation
636 of the precise metabolic pathways used by *H. salinarum* within halite brine inclusions will require
637 further analyses, overcoming the challenges of accessing the closed halite system.

638 **5.5.1.2 Similar Expression of DNA Repair, Replication, and Cell Division Proteins**

639 Acclimation to the halite brine inclusions microenvironment could presumably involve reduced or
640 silenced cell division, DNA replication and repair pathways. However, eight proteins involved in
641 chromosome partitioning were common to halite brine inclusions extracts and stationary growth phase
642 cultures, along with 11 other proteins involved in DNA replication including matches for DNA
643 primase, polymerase, gyrase, topoisomerase and replication factors. Only four DNA replication

644 proteins were found to be specific to stationary growth phase proteomes. This suggests that either such
645 proteins are constitutively expressed, or that DNA replication and cell division occur in a similar
646 fashion for both stationary growth phase cells and those within halite brine inclusions.

647 DNA repair processes were represented both within halite brine inclusions and liquid cultures
648 by the DNA photolyase, Rad50, the UvrD repair helicase, UvrA excinuclease, RadA recombinase,
649 Rad25 DNA repair helicase, Fen1 repair endonuclease and the Hel208 helicase are found shared
650 between liquids and brine extracts. Other DNA repair proteins were specific to either halite or liquid
651 samples. Stationary growth phase cultures contained additional repair proteins including the RmeR
652 site-specific deoxyribonuclease, endonuclease IV, RecJ single-strand exonuclease, MutL mismatch
653 repair protein, DNA gyrase and N-glycosylase, whereas the UvrB, MutS and endonuclease III proteins
654 were exclusive to halite brine inclusions proteomes.

655 **5.5.1.3 Shared Transcriptional Proteome But Reduced Translational Proteome**

656 Investigations of DNA transcription identified a shared proteome between liquid cultures and
657 brine inclusions including proteins for transcriptional initiation factors (TFIIE and TFIID) and
658 transcriptional machinery (RNA polymerase subunits rpoA2, rpoB1, rpoB2, rpoD and rpoE1). Proteins
659 involved in transfer RNA biogenesis such as tRNA ligases for 18 different amino acids along with two
660 ribonucleases completed the shared transcriptional proteome of liquid cultures cells and halite extracts.
661 Only tRNA ligases specific for tryptophan and threonine, four unique transcriptional proteins (rpoF,
662 rpoH, rpoN and nusA termination protein) and one unique transcription initiation factor (TFIIB) were
663 only found only in stationary growth phase cell extracts.

664 While early acclimation to the halite brine inclusions microenvironment resulted in nuanced
665 differences in the proteome of *H. salinarum* cells regarding cell division, replication, DNA repair and
666 transcriptional processes, stark differences were observed for proteins involved in translation activities.
667 Translational activities were severely restricted for cell within halite brine inclusions, as evidenced by
668 the down-regulation of 27 of the 42 ribosomal proteins shared by cells from both conditions tested.
669 Only one ribosomal protein was up-regulated. The shared proteome between cells in halite brine
670 inclusions and those in liquid culture included an additional 10 proteins involved in ribosome
671 biogenesis, and 10 translation initiation factors for which none showed any significant up- or down-
672 regulation. Chaperones proteins showed a high degree of conservation between conditions, with
673 thioredoxin, chaperone DnaJ, DnaK along with the GrPE stimulator, Hsp20, thermosome subunit and

674 prefoldin all shared by both liquid and halite extracts. Only prefoldin beta subunit was down-regulated
675 for cells from halite brine inclusions.

676 Taken together, these data indicate a high level of similarity between stationary growth phase
677 cells in liquid culture and those trapped within halite brine inclusions. Acclimation to the closed brine
678 inclusions microenvironment appears to severely limit translational activity. However, expressed
679 proteins are preserved indicating low levels of protein turnover. Cells maintain at least the capacity for
680 central metabolism, DNA repair, replication, and even cell division comparable to stationary growth
681 phase cells.

682 **5.5.2 Interactions Between Cells and the Brine Inclusions Microenvironment**

683 The potential interactions between *H. salinarum* cells and the local microenvironment within halite
684 brine inclusions focusing on cell surface and mobility processes involved in responses to external
685 stimuli.

686 **5.5.2.1 S-layer Maintained in Brine Inclusions**

687 Previous investigations on the survival of *Halobacterium* cells trapped within salt crystals have
688 proposed potential for cell envelope modifications with surface proteinaceous layer (S-layer) shed
689 (Fendrihan *et al*., 2012). However, this result seems to be the due to a lack of trace elements in the TN
690 buffer (4.28 M NaCl, Tris-HCl pH 7.4) used in the 2012 study, as argued by Kixmüller and Greie
691 (2012). The peptone added to the TNPA crystallization buffer used here provided sufficient trace
692 elements (including Mg, Ca, K) for S-layer maintenance and cell envelope function. S-layer shedding
693 within halite brine inclusions was previously thought to improve exchanges between cells and the local
694 microenvironment. However, in this study S-layer proteins were identified in all liquid culture and
695 halite samples without significant up- or down-regulation. This either indicates the S-layer is
696 maintained by *H. salinarum* cells, or that the S-layer proteins were preserved within the brine inclusion.
697 The fact that S-layer proteins quantities remained comparable to stationary phase cultures with intact
698 S-layers suggests that the S-layer proteins remain associated with *H. salinarum* cells within brine
699 inclusions.

700 **5.5.2.2 Increased Expression of Membrane Transporters**

701 Of the 20 membrane transporters shared between the proteomes of liquid cultures and cells
702 inside halite brine inclusions, four were found to be up-regulated in halite brine inclusions extract,
703 including the glycerol-3-phosphate-binding protein precursor. Moreover, six proteins were found to be

704 unique to the halite brine inclusions proteome including phosphate, iron and glycerol-3-phosphate
705 transporters. This suggests that transport capacity is not only maintained but enhanced in cells during
706 acclimation to halite brine inclusions, likely to maximize extraction of essential molecules and trace
707 elements from the local microenvironment. The upregulation of the glycerol-3-phosphate-binding
708 protein precursor may suggest a role for membrane lipid modification within brine inclusions.

709 **5.5.2.3 Modified Sensory Detection and Motility**

710 Previous published transcriptomics and proteomics studies on *H. salinarum* cell shown impact
711 of salinity and dissolved oxygen concentrations on motility (Schmid *et al*., 2007; Leuko *et al*., 2009).
712 We therefore examined the expression of archaellum, gas vesicles and chemotaxis proteins. A high
713 degree of variability was noted in the expression of these proteins between halite brine inclusions
714 extracts and stationary growth phase cultures. Some proteins were common to both proteomes without
715 any differences in protein quantities, including for the gas vesicle protein (Gvp) subunits F, C, N of
716 cluster A, while GvpA was found only in two of the four liquid cultures and two of four halite samples.
717 GvpD and I subunits of A cluster and F of B cluster were found punctually in liquid samples. Only
718 GvpO cluster A and B seems to be impacted by crystallization with significant down-regulation in
719 halite brine inclusions extracts. A similar down-regulation of *gvpO* mRNA was observed in response
720 to UV irradiation (Baliga *et al.,* 2004), and GvpO protein expression levels after exposure to ionizing
721 radiation (Webb *et al.*, 2013). Lack of the GvpO gas vesicle expression regulator is thought to inhibit
722 gas vesicle formation, and growth by anoxic arginine fermentation is also known to reduce the number
723 of gas vesicles in *H. salinarum* NRC-1 (Hechler and Pfeifer, 2009).

724 For the archaellum proteins, only archaellin B1 was down-regulated in halite samples whereas
725 achaellin A1 and prearchaellin peptidase were identified punctually in liquid culture samples.
726 Archaellin B2, A2 and flagellin related H protein were found in all liquid culture replicates but only in
727 one halite replicate. An examination of chemotaxis proteins showed that the 18 identified proteins
728 including CheR, CheA, CheW, CheC, CheB, and the methyl-accepting chemotaxis (MCP)-family
729 proteins Htr transducers, were shared between halite brine inclusions extract and stationary growth
730 phase liquid cultures. The expression of multiple transducer proteins is often correlated with changing
731 environmental conditions, and in this case may be the remanent proteins from the acclimation of *H.*
732 *salinarum* to halite brine inclusions.

733 The bacterio-opsin activator-like protein, along both sensory rhodopsins (I and II) and their
734 accompanying Htr signal transducers were common to all conditions and replicates. This indicates that

detection of more damaging blue and UV light as part of phototaxis remains functional both prior to and after evaporation of *H. salinarum* cultures. In contrast, while bacterio-opsin activator (Boa1; AAG18778.1) was only found in two of the four halite brine inclusions replicate samples. While this protein is hypothesized to be a DNA-binding transcriptional regulator in the photosensory network, its role remains unconfirmed.

These data show a general down-regulation of archaellin proteins involved in motility for cells in brine inclusions compared to stationary phase liquid cultures. So while chemo- and photo-taxis proteins are maintained in brine inclusions, the accompanying archaellum motility is not. A reduced motility may be induced in halite brine inclusions to preserve energy. Gas vesicle down-regulation suggests a lack of needed capacity for vertical movement in a water column in response to oxygen levels, consistent with the restricted confines of a microscopic halite brine inclusions. Although no swim or floating occur for brine inclusions, cells remain able to receive environmental signals through chemotaxis and photosensory proteins founded both in stationary cells and brine inclusion extracts without significant differential expression.

6 Conclusion

This is the first study that demonstrate the possibility to isolate proteins directly and efficiently from halite brine inclusions while simultaneously excluding surface-bound contaminating proteins and avoiding changes in cell protein expression during salt dissolution. Also, this work provides the first insights into the molecular mechanisms involved in the early acclamation of *H. salinarum* within brine inclusions. Based on our findings, the cells of *H. salinarum* appear to be in a low activity 'maintenance' or 'semi-dormant' state, similar to other bacteria and archaea in low-energy environments such as the deep biosphere (reviewed in Lever *et al.,* 2015). Whether or not *H. salinarum* cells inside brine inclusions are true 'persister' cells (Megaw and Gilmore, 2017) will require future study. Despite the reasonable assumption brine inclusions represent stress conditions for *Halobacterium* cells, no increased expression of stress-response proteins such as chaperones was observed. The acclimation to the halite environment may therefore be less a stress response than a reduction in cell activity.

Shifts in the proteome of *H. salinarum* NRC-1 have been studied using liquid cultures under conditions similar to those thought to exist inside halite brine inclusions: reduced oxygen content (Schmid *et al.* 2007), increased salinity (Leuko *et al.,* 2008), and transitions from aerobic to anaerobic growth (Tebbe *et al.,* 2009). While the down-regulation of certain ribosomal proteins and archaellum precursors was also observed following salinity stress (Leuko *et al.,* 2008) not all protein expression

shifts conformed to this pattern. The same was observed for the transition from aerobic to anaerobic growth, with increased expression of the arginine deaminase as observed by Tebbe *et al.* (2009) but other protein expression differences due to the use of culturing conditions that were not identical to those in previous studies. Thus, while proteomics analyses from liquid cultures can provide hints to aid in the interpretation of the data presented here, they can not fully explain the observed patterns of protein expression within halite brine inclusions.

The unique environment of halite brine inclusions limits exchange of nutrients between cells and their surrounding environment. It also allows for the buildup of toxic metabolic waste products which appear to limit the duration of cell viability within the brine inclusions. Further functional investigations are clearly needed to confirm the hypotheses generated by proteomics data in this study, particularly in regards to cell activity. While this study does not resolve the question of how long microorganisms are able to retain viability within halite brine inclusions, it offers clear insights into the process of early microbial acclimation to evaporation of hypersaline environments in halophilic archaea. The methodologies presented here will also enable future study of the biomolecules of microorganisms in halite inclusions in natural settings, particularly small-sized halite crystals.

7 Data Availability Statement

Proteomics data are available to the ProteomeXchange Consortium via the PRIDE partner repository with the dataset identifier PXD037167 and 10.6019/PXD037167.

8 Author Contributions

Study was designed by CF, AK, AH and SZ under supervision of AK, SZ and AH. Experiments were conducted by CF with the help of MM for crystals forming; AM and RP for mass spectrometry and improvements of extraction methods; BAB for nanoLC-MS/MS data acquisition; FG for MEB-EDX analyses; AT for RNA extraction and TD for plasma treatments. Proteomics data treatments were conducted by AT and CF. Manuscript was written by CF and then revised and approved by all co-authors.

9 Acknowledgments

This work was supported by the X-life program of CNRS-MITI, the ATM program of the Muséum National d'Histoire Naturelle, the French National Research Agency ANR-PRCI "ExocubeHALO" project (ANR-21-CE49-0017-01_ACT), and the Sorbonne Université (graduate stipend C. Favreau).

UHPLC MS/MS data were acquired at the Plateau Technique de Spectrométrie de Masse Bio-organique, UMR 7245 Molécules de Communication et d'Adaptation des Microorganismes, Muséum national d'Histoire naturelle, Paris, France. The nanoLC-MS/MS data were acquired at ProGenoMix MS-platform at CEA-Marcoule. Thanks to Imène Esteve of the FIB and SEM facility of IMPMC which was supported by Région Ile de France Grant SESAME 2006 NOI-07-593/R, Institut National des Sciences de l'Univers (INSU)–CNRS, Institut de Physique–CNRS, Sorbonne Université, and the French National Research Agency (ANR) grant ANR-07-BLAN-0124-01. Parts of figures used images from Servier Medical Art. Servier Medical Art by Servier is licensed under a Creative Commons Attribution 3.0 Unported License (https://creativecommons.org/licenses/by/3.0/).

10 Supplementary

Supplementary Information for this article are available online.

11 References

Baliga, N. S., Bjork, S. J., Bonneau, R., Pan, M., Iloanusi, C., Kottemann, M. C. H., et al. (2004). Systems Level Insights Into the Stress Response to UV Radiation in the Halophilic Archaeon Halobacterium NRC-1. *Genome Res* 14, 1025–1035. doi: 10.1101/gr.1993504.

Bidle, K. A., Kirkland, P. A., Nannen, J. L., and Maupin-Furlow, J. A. (2008). Proteomic analysis of *Haloferax volcanii* reveals salinity-mediated regulation of the stress response protein PspA. Microbiol Read Engl 154, 1436–43. doi: 10.1099/mic.0.2007/015586-0.

Coker, J. A., DasSarma, P., Kumar, J., Müller, J. A., and DasSarma, S. (2007). Transcriptional profiling of the model Archaeon *Halobacterium* sp. NRC-1: responses to changes in salinity and temperature. Saline Syst 3, 6. doi: 10.1186/1746-1448-3-6.

Eichler, J. (2019). Halobacterium salinarum. *Trends Microbiol* 27, 651–652. doi: 10.1016/j.tim.2019.02.005.

Engel, M. B., and Catchpole, H. R. (2005). A microprobe analysis of inorganic elements in *Halobacterium salinarum*. Cell Biol Int 29, 616–622. doi: 10.1016/j.cellbi.2005.03.024.

Falb, M., Müller, K., Königsmaier, L., Oberwinkler, T., Horn, P., Gronau, S. von, et al. (2008). Metabolism of halophilic archaea. Extremophiles 12, 177–196. doi: 10.1007/s00792-008-0138-x.

Fendrihan, S., Dornmayr-Pfaffenhuemer, M., Gerbl, F. W., Holzinger, A., Grösbacher, M., Briza, P., et al. (2012). Spherical particles of halophilic archaea correlate with exposure to low water activity – implications for microbial survival in fluid inclusions of ancient halite. Geobiology 10, 424–433. doi: 10.1111/j.1472-4669.2012.00337.x.

Gonzalez, O., Gronau, S., Pfeiffer, F., Mendoza, E., Zimmer, R., and Oesterhelt, D. (2009). Systems Analysis of Bioenergetics and Growth of the Extreme Halophile *Halobacterium salinarum*. Plos Comput Biol 5, e1000332. doi: 10.1371/journal.pcbi.1000332.

Gramain, A., Díaz, G. C., Demergasso, C., Lowenstein, T. K., and McGenity, T. J. (2011). Archaeal diversity along a subterranean salt core from the Salar Grande (Chile). Environ Microbiol 13, 2105–2121. doi: 10.1111/j.1462-2920.2011.02435.x.

Graur, D., and Pupko, T. (2001). The Permian Bacterium that Isn't. *Mol Biol Evol* 18, 1143–1146. doi: 10.1093/oxfordjournals.molbev.a003887.

Thomas, C., Grossi, V., Antheaume, I., and Ariztegui, D. (2019). Recycling of archaeal biomass as a new strategy for extreme life in Dead Sea deep sediments. *Geology* 47, 479–482. doi: 10.1130/g45801.1.

Gruber, C., Legat, A., Pfaffenhuemer, M., Radax, C., Weidler, G., Busse, H.-J., et al. (2004). *Halobacterium noricense* sp. nov., an archaeal isolate from a bore core of an alpine Permian salt deposit, classification of *Halobacterium* sp. NRC-1 as a strain of *H. salinarum* and emended description of *H. salinarum*. Extremophiles 8, 431–439. doi: 10.1007/s00792-004-0403-6.

Hartmann, R., Sickinger, H. D., and Oesterhelt, D. (1980). Anaerobic growth of halobacteria. Proc National Acad Sci 77, 3821–3825. doi: 10.1073/pnas.77.7.3821.

Hechler, T., and Pfeifer, F. (2009). Anaerobiosis inhibits gas vesicle formation in halophilic Archaea. *Molecular Microbiology* 71, 132–145. doi: 10.1111/j.1365-2958.2008.06517.x.

Huby, T. J. C., Clark, D. R., McKew, B. A., and McGenity, T. J. (2020). Extremely halophilic archaeal communities are resilient to short-term entombment in halite. Environ Microbiol. doi: 10.1111/1462-2920.14913.

Judée, F., Simon, S., Bailly, C., and Dufour, T. (2018). Plasma-activation of tap water using DBD for agronomy applications: Identification and quantification of long lifetime chemical species and production/consumption mechanisms. Water Res 133, 47–59. doi: 10.1016/j.watres.2017.12.035.

Kanehisa, M., and Goto, S. (2000). KEGG: Kyoto Encyclopedia of Genes and Genomes. Nucleic Acids Res 28, 27–30. doi: 10.1093/nar/28.1.27.

Kanehisa, M., Sato, Y., and Morishima, K. (2016). BlastKOALA and GhostKOALA: KEGG Tools for Functional Characterization of Genome and Metagenome Sequences. J Mol Biol 428, 726–731. doi: 10.1016/j.jmb.2015.11.006.

Kirkland, P. A., Busby, J., Stevens, S., and Maupin-Furlow, J. A. (2006). Trizol-based method for sample preparation and isoelectric focusing of halophilic proteins. Anal Biochem 351, 254–259. doi: 10.1016/j.ab.2006.01.017.

Kixmüller, D., and Greie, J. (2012). An ATP-driven potassium pump promotes long-term survival of Halobacterium salinarum within salt crystals. Env Microbiol Rep 4, 234–241. doi: 10.1111/j.1758-2229.2012.00326.x.

Leuko, S., Raftery, M. J., Burns, B. P., Walter, M. R., and Neilan, B. A. (2009). Global Protein-Level Responses of *Halobacterium salinarum* NRC-1 to Prolonged Changes in External Sodium Chloride Concentrations. J Proteome Res 8, 2218–2225. doi: 10.1021/pr800663c.

Lever, M. A., Rogers, K. L., Lloyd, K. G., Overmann, J., Schink, B., Thauer, R. K., et al. (2015). Life under extreme energy limitation: a synthesis of laboratory- and field-based investigations. *Fems Microbiol Rev* 39, 688–728. doi: 10.1093/femsre/fuv020.

Maughan, H., Birky, W., Nicholson, W., Rosenzweig, W., and Vreeland, R. (2002). The paradox of the "ancient" bacterium rich contains "modern" protein-coding genes.

Megaw, J., and Gilmore, B. F. (2017). Archaeal Persisters: Persister Cell Formation as a Stress Response in Haloferax volcanii. *Frontiers in microbiology* 8, 1589. doi: 10.3389/fmicb.2017.01589.

Merino, N., Aronson, H. S., Bojanova, D. P., Feyhl-Buska, J., Wong, M. L., Zhang, S., et al. (2019). Living at the Extremes: Extremophiles and the Limits of Life in a Planetary Context. Front Microbiol 10, 780. doi: 10.3389/fmicb.2019.00780.

Moran-Reyna, A., and Coker, J. A. (2014). The effects of extremes of pH on the growth and transcriptomic profiles of three haloarchaea. F1000research3, 168. doi: 10.12688/f1000research.4789.2.

Mormile, M. R., Biesen, M. A., Gutierrez, M. C., Ventosa, A., Pavlovich, J. B., Onstott, T. C., et al. (2003). Isolation of *Halobacterium salinarum* retrieved directly from halite brine inclusions. Environ Microbiol 5, 1094–1102. doi: 10.1046/j.1462-2920.2003.00509.x.

Müller, J. A., and DasSarma, S. (2005). Genomic Analysis of Anaerobic Respiration in the Archaeon *Halobacterium* sp. Strain NRC-1: Dimethyl Sulfoxide and Trimethylamine N-Oxide as Terminal Electron Acceptors. J Bacteriol 187, 1659–1667. doi: 10.1128/jb.187.5.1659-1667.2005.

Nickle, D. C., Learn, G. H., Rain, M. W., Mullins, J. I., and Mittler, J. E. (2002). Curiously Modern DNA for a "250 Million-Year-Old" Bacterium. J Mol Evol 54, 134–137. doi: 10.1007/s00239-001-0025-x.

Nims, C., Lafond, J., Alleon, J., Templeton, A. S., and Cosmidis, J. (2021). Organic biomorphs may be better preserved than microorganisms in early Earth sediments. Geology 49, 629–634. doi: 10.1130/g48152.1.

Norton, C. F., and Grant, W. D. (1988). Survival of Halobacteria Within Fluid Inclusions in Salt Crystals. Journal of General Microbiology, 1365–1373.

Oesterhelt, D., and Stoeckenius, W. (1974). Methods in Enzymology. Methods Enzymol 31, 667–678. doi: 10.1016/0076-6879(74)31072-5.

Oren, A., Arahal, D. R., and Ventosa, A. (2009). Emended descriptions of genera of the family Halobacteriaceae. Int J Syst Evol Micr 59, 637–642. doi: 10.1099/ijs.0.008904-0.

Oren, A. (2006). Life at high salt concentrations. The prokaryotes 3, 263–282. doi: 10.1007/0-387-30742-7-9.

Payne, J. I., Sehgal, S. N., and Gibbons, N. E. (1960). Immersion Refractometry of some halophilic bacteria. Can J Microbiol 6, 9–15. doi: 10.1139/m60-002.

Pinel-Cabello, M., Chapon, V., Ruiz-Fresneda, M. A., Alpha-Bazin, B., Berthomieu, C., Armengaud, J., et al. (2021). Delineation of cellular stages and identification of key proteins for reduction and biotransformation of Se(IV) by Stenotrophomonas bentonitica BII-R7. J Hazard Mater 418, 126150. doi: 10.1016/j.jhazmat.2021.126150.

Podechard, N., Ducheix, S., Polizzi, A., Lasserre, F., Montagner, A., Legagneux, V., et al. (2018). Dual extraction of mRNA and lipids from a single biological sample. Sci Rep-uk 8, 7019. doi: 10.1038/s41598-018-25332-9.

Post, F. J. (1977). The microbial ecology of the Great Salt Lake. Microbial Ecol 3, 143–165. doi: 10.1007/bf02010403.

Roedder, E. (1984). The fluids in salt. American Mineralogist 69, 413–439.

Rosenzweig, W. D., Peterson, J., Woish, J., and Vreeland, R. H. (2000). Development of a Protocol to Retrieve Microorganisms from Ancient Salt Crystals. Geomicrobiol J 17, 185–192. doi: 10.1080/01490450050121152.

Sankaranarayanan, K., Timofeeff, M. N., Spathis, R., Lowenstein, T. K., and Lum, J. K. (2011). Ancient Microbes from Halite Fluid Inclusions: Optimized Surface Sterilization and DNA Extraction. Plos One 6, e20683. doi: 10.1371/journal.pone.0020683.

Schmid, A. K., Reiss, D. J., Kaur, A., Pan, M., King, N., Van, P. T., et al. (2007). The anatomy of microbial cell state transitions in response to oxygen. *Genome Research* 17, 1399–1413. doi: 10.1101/gr.6728007.

Schmid, A. K., Reiss, D. J., Pan, M., Koide, T., and Baliga, N. S. (2009). A single transcription factor regulates evolutionarily diverse but functionally linked metabolic pathways in response to nutrient availability. Mol Syst Biol 5, 282. doi: 10.1038/msb.2009.40.

Schreder-Gomes, S. I., Benison, K. C., and Bernau, J. A. (2022). 830-million-year-old microorganisms in primary fluid inclusions in halite. Geology. doi: 10.1130/g49957.1.

Shimizu, S., Barczyk, S., Rettberg, P., Shimizu, T., Klaempfl, T., Zimmermann, J. L., et al. (2014). Cold atmospheric plasma – A new technology for spacecraft component decontamination. Planet Space Sci 90, 60–71. doi: 10.1016/j.pss.2013.10.008.

Tebbe, A., Schmidt, A., Konstantinidis, K., Falb, M., Bisle, B., Klein, C., et al. (2009). Life-style changes of a halophilic archaeon analyzed by quantitative proteomics. Proteomics 9, 3843–3855. doi: 10.1002/pmic.200800944.

Vreeland, R. H., Rosenzweig, W. D., and Powers, D. W. (2000). Isolation of a 250 million-year-old halotolerant bacterium from a primary salt crystal. Nature 407, 897–900. doi: 10.1038/35038060.

Webb, K. M., Yu, J., Robinson, C. K., Noboru, T., Lee, Y. C., and DiRuggiero, J. (2013). Effects of intracellular Mn on the radiation resistance of the halophilic archaeon Halobacterium salinarum. *Extremophiles* 17, 485–497. doi: 10.1007/s00792-013-0533-9.

Winters, Y. D., Lowenstein, T. K., and Timofeeff, M. N. (2015). Starvation-Survival in Haloarchaea. Life 5, 1587–1609. doi: 10.3390/life5041587.

12 Table and Figures

Table 1: Experimental parameters of cold plasma sources used to remove surface-bound proteins. Proteolysis was measured as a percentage of total proteins removed (as determined by modified BCA assay) compared to untreated halite. DBD means dielectric barrier device; APPJ for atmospheric pressure plasma jet. The abbreviations 'slm' and 'sccm' are used for standard liters per minute and sccm standard centimeters cube per minute, respectively.

Plasma source	Excitation mode	Electrical parameters			Gas and flow rate	Proteolysis
		Ampl.	Freq.	Duty cycle		
DBD	Alternative Current	7 kV	500 Hz	-	He (1 slm)	0.0 %
					He-O_2 (1slm - 150 sccm)	0.0 %
					He-O_2 (1slm - 3 sccm)	0.0 %
					Ar (1 slm)	0.0 %
APPJ	Alternative Current	7 kV	700 Hz	-	He (6 slm)	0.0 %
	Pulse	7 kV	700 Hz	1 %	He (6 slm)	29.3 %
					He-O_2 (6 slm - 100 sccm)	39.1 %

Table 2: Total purified RNA quality check results after TRIzol Reagent™ -based extraction. [a]See Supplementary Figure 6-2 for BioAnalyzer results. Purity score below 2.0 suggest purity unsuitable for RNAseq analyses.

	Liquid stationary cells			Internally inoculated halite (2 months)			Externally inoculated halite (~1 week)		
RNA quantity (µg)	1040.0	1045.2	1190.8	<20	4.4	13.9	327.6	444.0	129.6
Purity (absorbance 260/280nm)	2.10	2.09	2.08	1.95	1.54	1.61	1.99	2.03	1.98
Purity (absorbance 260/230nm)	2.44	2.38	2.47	4.67	0.96	1.44	1.89	1.78	2.05
Quality[a]	+	++	++	--	--	--	-	-	-

949 **Figure 1**: TNPA laboratory-grown halite crystals internally inoculated with *Halobacterium salinarum*
950 cells observed after two months of incubation at 37 °C for crystallization replicates 1-3 (A-C,
951 respectively).

952 **Figure 2**: Laboratory-grown halite surface observation. (A-F) TNPA crystals without cells. (G-J)
953 Internally inoculated TNPA crystals with *Halobacterium salinarum* cells incubated two months at 37
954 °C. (K-N) Externally inoculated TNPA crystals with *Halobacterium salinarum* cells after
955 approximately one week incubated at 37 °C. (A, G, K) Schematic representation of halite crystals
956 without cells, internally inoculated and externally inoculated respectively. (B, H, L) Visual observation
957 of crystals without cells, internally inoculated and externally inoculated, respectively. (C, E) Secondary
958 electron images. (I, M) Backscattered images. (D, F, J, N) Elemental composition analysis by EDX
959 spectroscopy correlated respectively to the SEM images in panels C, E, I, and M.

960 **Figure 3**: Surface-bounded protein removal by chemical treatments with active-spray washes. (A)
961 Percentage of proteins removed after NaOCl-NaOH treatment with or without an additional HCl
962 treatment step, and subsequent residual protein quantity. (B) Overview of optimal NaOCl-NaOH-HCl
963 chemical treatment with active-spray washes.

964 **Figure 4**: Venn diagrams of proteins identified by mass spectrometry for brine inclusions and liquid
965 stationary culture samples. (A) Comparison of biological replicates for liquid stationary culture
966 extracts. B) Comparison of biological replicates for brine inclusions extracts. Black circles in (A) and
967 (B) represent "core" proteins shared by the four replicates in both cases. (C) Comparison of core
968 proteins between brine inclusion extracts and liquid stationary culture cells.

969 **Figure 5**: Venn diagram of the 68 proteins quantified by iTRAQ® with triple injection which exhibit
970 significative differential expression in brine extracts compared to liquid stationary culture cells.

971 **Figure 6**: Schematic overview of targets cellular functions involved in early acclimation of
972 *Halobacterium salinarum* through halite brine inclusions (for extended matched proteins, see
973 Supplementary Table 6-5). Shared (*) indicates proteins found in all four brine inclusion extracts and
974 all four liquid stationary culture extracts. Partially shared (**) indicates proteins found in both brine
975 inclusions and stationary phase liquid culturs, but not for all replicate samples for each condition.

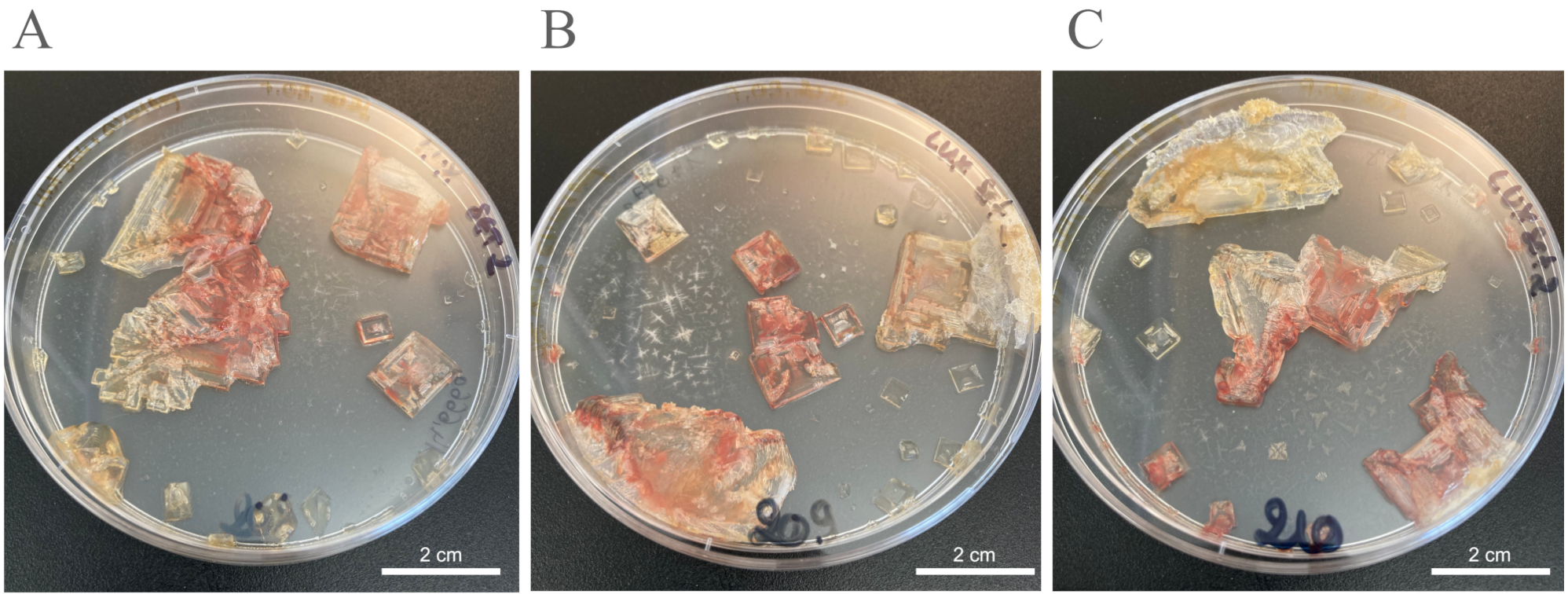
A
B
C
2 cm
2 cm
2 cm

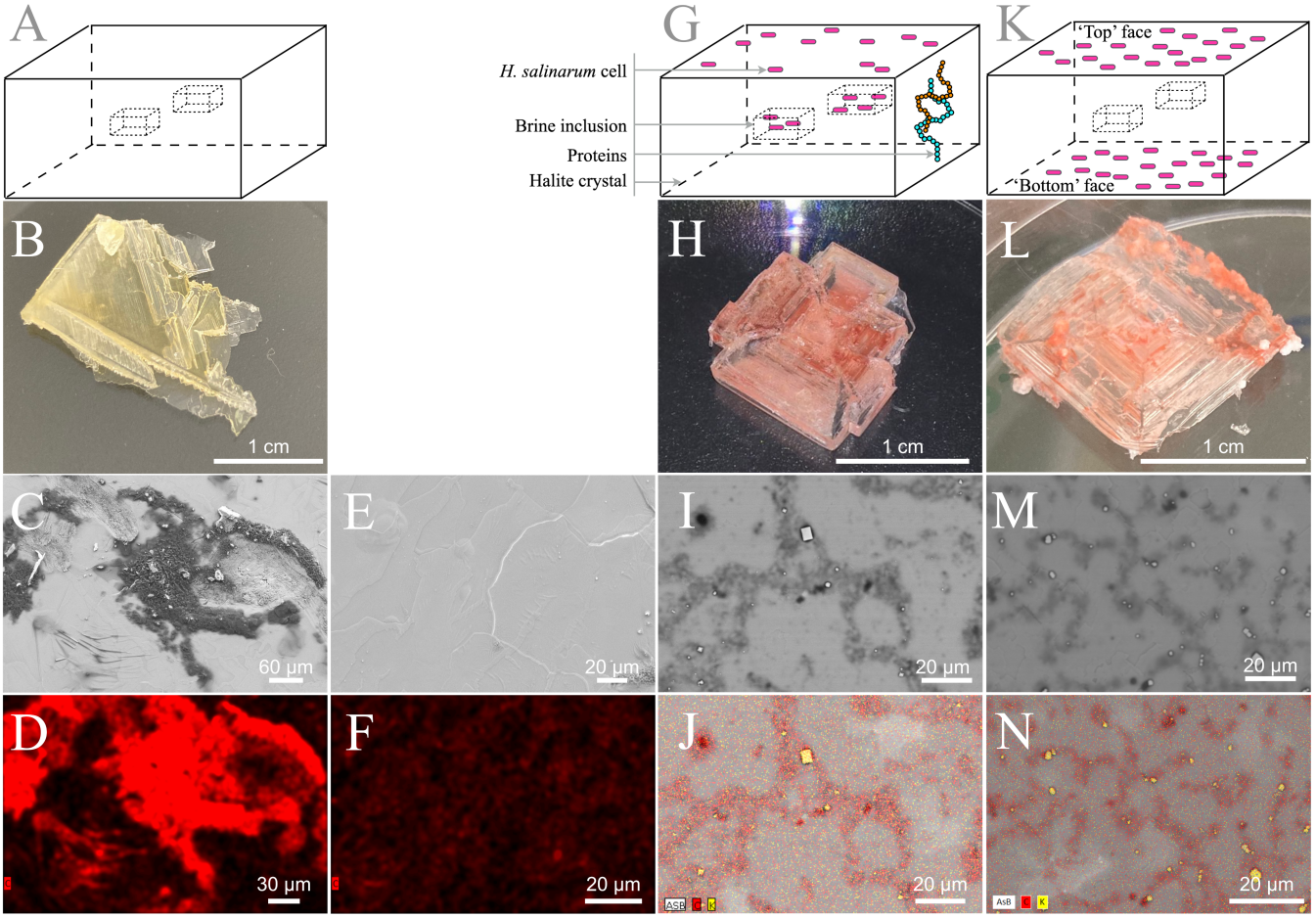
A
G
K
H. salinarum cell
Brine inclusion
Proteins
Halite crystal
'Top' face
'Bottom' face
B
H
L
1 cm
1 cm
1 cm
C
E
I
M
60 µm
20 µm
20 µm
20 µm
D
F
J
N
30 µm
20 µm
20 µm
20 µm
AsB
Cl
K
AsB
Cl
K

A

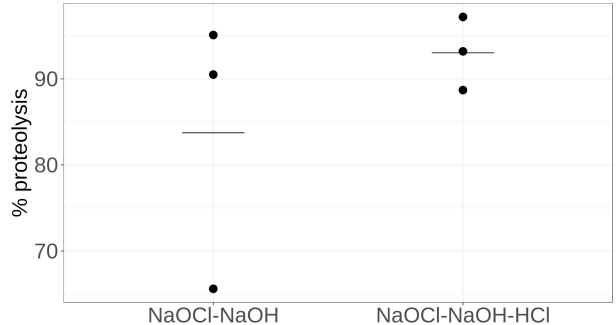
% proteolysis
90
80
70
NaOCl-NaOH
NaOCl-NaOH-HCl

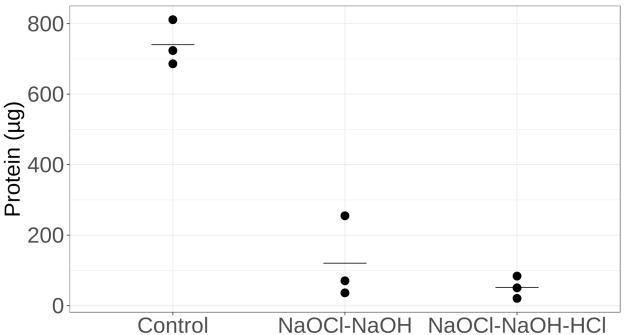
Protein (µg)
800
600
400
200
0
Control
NaOCl-NaOH
NaOCl-NaOH-HCl

B

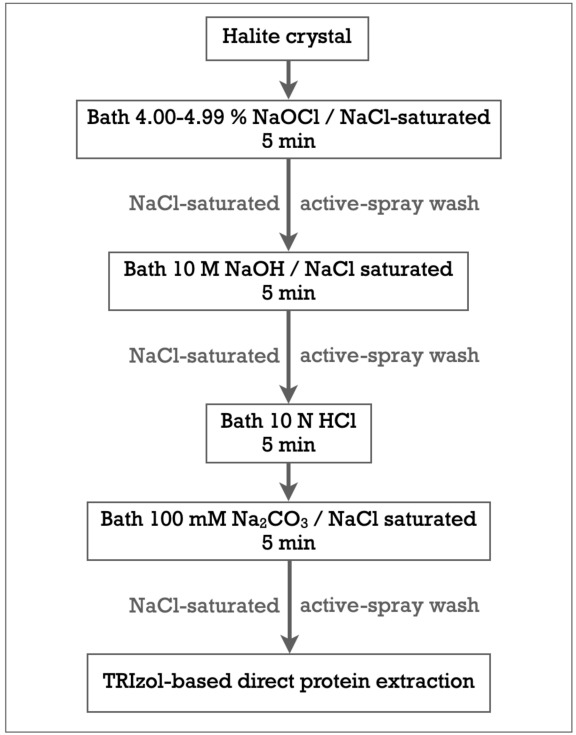
Halite crystal
Bath 4.00-4.99 % NaOCl / NaCl-saturated
5 min
NaCl-saturated
active-spray wash
Bath 10 M NaOH / NaCl saturated
5 min
NaCl-saturated
active-spray wash
Bath 10 N HCl
5 min
Bath 100 mM Na_2CO_3 / NaCl saturated
5 min
NaCl-saturated
active-spray wash
TRIzol-based direct protein extraction

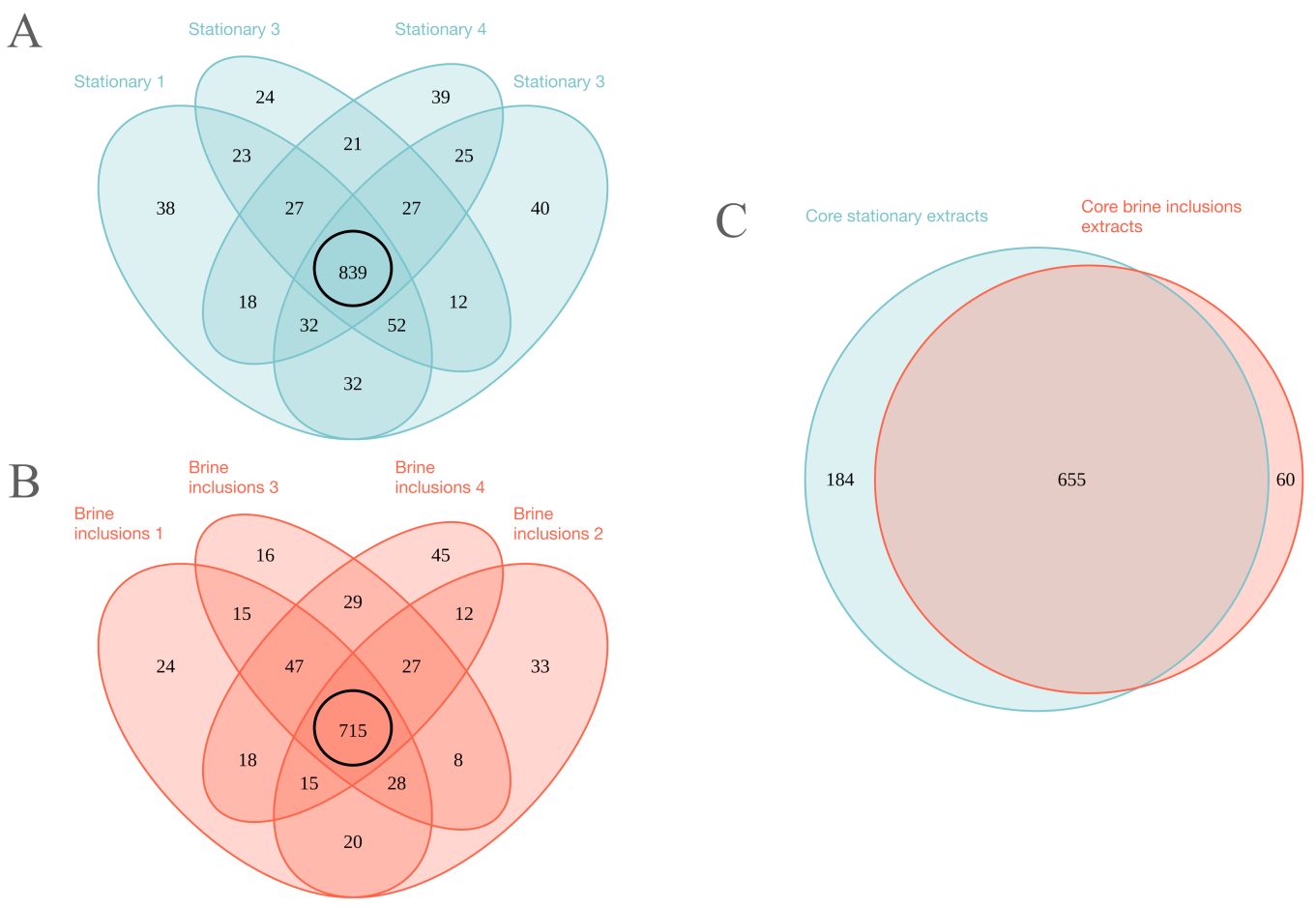
A
Stationary 1
Stationary 3
Stationary 4
Stationary 3
24
39
21
23
25
38
27
27
40
839
18
12
32
52
32
B
Brine inclusions 1
Brine inclusions 3
Brine inclusions 4
Brine inclusions 2
16
45
29
15
12
24
47
27
33
715
18
8
15
28
20
C
Core stationary extracts
Core brine inclusions extracts
184
655
60

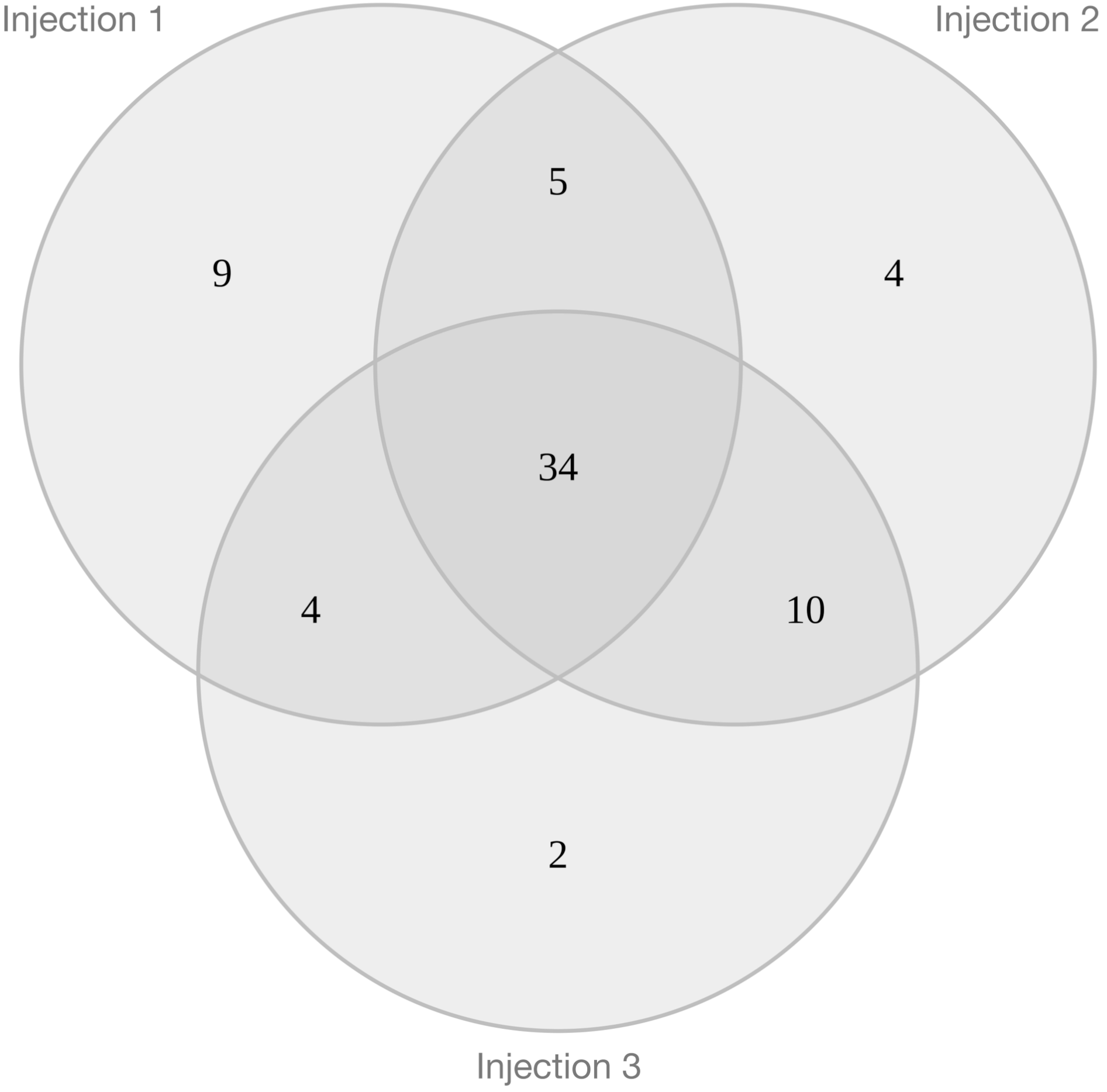
Injection 1
Injection 2
Injection 3
9
5
4
34
4
10
2

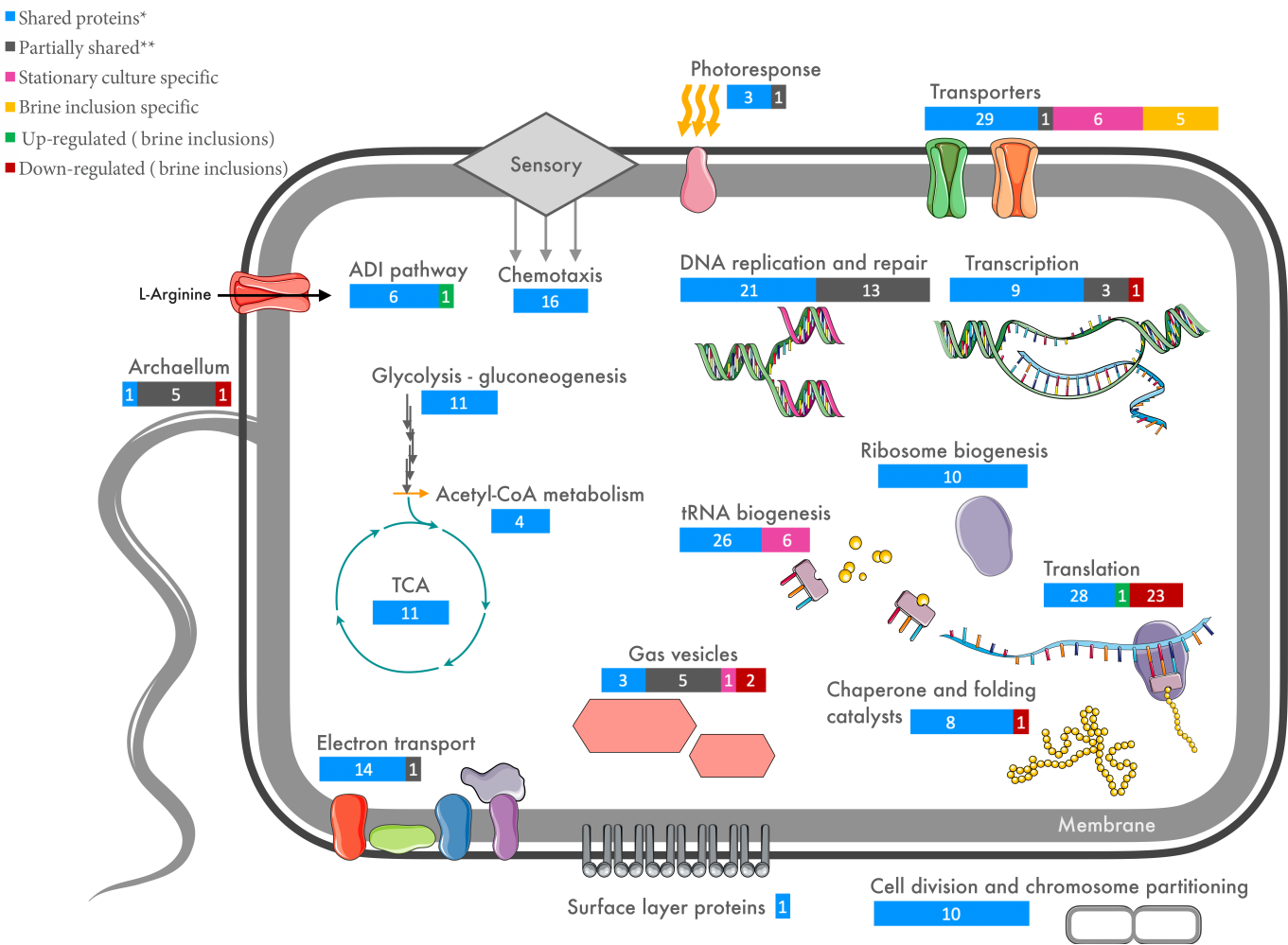
Shared proteins*
Partially shared**
Stationary culture specific
Brine inclusion specific
Up-regulated (brine inclusions)
Down-regulated (brine inclusions)
Photoresponse
3 1
Transporters
29 1 6 5
Sensory
Chemotaxis
16
L-Arginine
ADI pathway
6 1
DNA replication and repair
21 13
Transcription
9 3 1
Archaellum
1 5 1
Glycolysis - gluconeogenesis
11
Ribosome biogenesis
10
Acetyl-CoA metabolism
4
tRNA biogenesis
26 6
TCA
11
Translation
28 1 23
Gas vesicles
3 5 1 2
Chaperone and folding catalysts
8 1
Electron transport
14 1
Membrane
Surface layer proteins 1
Cell division and chromosome partitioning
10